EXPRESSION, PHARMACOLOGICAL AND PHYSIOLOGICAL PROPERTIES OF NICOTINIC ACETYLCHOLINE RECEPTORS

by

Olena Filchakova

A dissertation submitted to the faculty of
The University of Utah
in partial fulfillment of the requirements for the degree of

Doctor of Philosophy

Neuroscience Program

The University of Utah

August 2013

The University of Utah Graduate School

STATEMENT OF DISSERTATION APPROVAL

The dissertation of **Olena Filchakova**

has been approved by the following supervisory committee members:

J. Michael McIntosh	, Chair	**05/21/2013** Date Approved
Baldomero Olivera	, Member	**05/21/2013** Date Approved
Doju Yoshikami	, Member	**05/21/2013** Date Approved
Michael Sanguinetti	, Member	**05/22/2013** Date Approved
Karen Wilcox	, Member	**05/22/2013** Date Approved

and by **Kristen Keefe** , Chair of the Department of **Neuroscience**

and by Donna M. White, Interim Dean of The Graduate School.

ABSTRACT

Nicotinic acetylcholine receptors are ligand-gated ion channels. These receptors play important roles in physiological as well as pathophysiological processes. The present work was aimed at studying three questions that were centered on pharmacology, expression and physiology of nicotinic receptors.

The first chapter describes the results of work that was aimed at understanding the molecular determinants of interaction between α-conotoxin BuIA and complementary subunits of nicotinic acetylcholine receptors. Proline 6 of BuIA was found to be a major determinant of binding to nAChR β2 subunit. Coupling between proline 6 and the residue at 59^{th} position of the β subunit was found to be equal to 2.4 kcal/mol. This work paves the ground for creating selective ligands that discriminate between α3β2 and α3β4 receptors.

The second chapter describes the dependence of expression of human α9-containing nicotinic acetylcholine receptors in the *Xenopus laevis* oocyte expression system on the 5'leader sequence of the α9 subunit. The human α9 subunit was determined to be the limiting factor in the functional expression of α9-containing receptors. The inclusion of the 5'leader from alfalfa mosaic virus before the α9 coding sequence facilitated the expression of human α9 homomeric receptors by ~70 fold and human α9α10 receptors by ~80 fold. As a result, a vector was created that allowed high

expression levels of α9-containing nAChRs; this advance allows reliable testing of new compounds that target human α9-containing receptors.

The third chapter describes results of work aimed at understanding the interaction between rat nicotinic α9α10 and purinergic receptors. Comparison of currents from coactivation of receptors to the predicted currents gave inconclusive results. Comparison of agonist sensitivities for purinergic receptors when receptors are expressed alone and when they are coinjected revealed ~1.6-fold difference in sensitivity, with P_2X_4 receptors less sensitive to ATP when α9α10 receptors are coexpressed. Interactions between rat α9α10 nicotinic receptor and purinergic P_2X_7 receptors were also examined and yielded negative results.

CONTENTS

LIST OF TABLES

LIST OF FIGURES

Figure

CHAPTER 1

INTERACTION BETWEEN α-CONOTOXIN BuIA AND THE β-SUBUNIT OF NICOTINIC ACETYLCHOLINE RECEPTORS

Introduction

Neuronal nicotinic acetylcholine receptors (nAChRs) together with $GABA_A$, GABAc, glycine, and 5-HT3 receptors belong to the group of ligand-gated ion channels. In the mammalian genome eleven neuronal nAChR subunits genes have been identified (α2-α7, α9-α10, and β2-β4). Functional neuronal nAChRs are homo- or heteropentamers. α7 and α9 subunits are able to assemble as homopentamers, α2-α6 subunits require β2-β4 subunits to make heteropentamers, α10 forms a heteromer with α9 (1,2). Neuronal nicotinic acetylcholine receptors are found in various neuronal and non-neuronal tissues and organs. In the central and peripheral nervous systems, neuronal nAChRs are found at presynaptic and postsynaptic sites and they contribute both to neurotransmission and modulation of release of several neurotransmitters including dopamine, glutamate and GABA (3). Non-neuronal localizations of neuronal nAChRs include keratinocytes, cochlear hair cells, lymphoid tissue, macrophages, epithelial cells in airways, vascular tissue, astrocytes and placenta (4,5).

Due to such broad representation throughout the organism, nAChRs have been implicated in a range of physiological and pathophysiological functions related to cognition, reward, arousal, learning and memory, motor control, antinociception, immune function and nicotine addiction (6,7). Unfortunately, the rational design of selective ligands to target a particular receptor subtype is challenging due to several factors. First, there is considerable conservation of nAChR residues (among different subunits) that form the ligand-binding sites. Second, the three-dimensional structure of the ligand binding site of nAChRs is not fully resolved. Current knowledge about the structure of the nAChR and its ligand-binding domain is largely derived from electron microscopy of

the muscle nAChR from an electric organ of *Torpedo californica* (8) and the crystal structure of the ACh-binding protein (AChBP), a soluble protein expressed by glial cells of fresh water snails. Although detailed models of neuronal nAChRs have been constructed based on these structures, these models may not fully account for known ligand activity (9). Third, many ligands show poor selectivity toward a particular receptor subtype. For example, antagonists mecamylamine and dihidro-β-erythroidine do not discriminate well among different heteromeric neuronal nAChRs.

Small disulfide rich peptides known as conotoxins found in the venom of predatory *Conus* snails have facilitated the search for and rational design of selective ligands. Conotoxins have among their targets different voltage and ligand gated ion channels, GPCRs, and norepinephrine transporters (10). α-Conotoxins target nAChRs (11,12), and compete with ACh at its binding site, which is formed at the interface between neighboring subunits. Some α-conotoxins show preference toward a particular nAChR subtype. For example, α-conotoxin ImI selectively blocks α7 and α3β2 nAChRs (13,14), α-conotoxin MII shows high selectivity for α6β2 and α3β2 nAChRs (15,16), and α-conotoxin RgIA targets α9α10 nAChRs (17).

α-conotoxin BuIA is a structurally unique 13 amino acid peptide with α-4/4 Cys spacing (number of residues between cysteine residues). Interestingly, α-conotoxin BuIA can kinetically discriminate between nAChRs that contain a β2 vs. β4 subunit; the off-rate for all β4- containing nAChRs is slow compared to all corresponding β2-containing nAChR subtypes (18). We previously identified residue differences between α3β2 and α3β4 nAChRs that interact with BuIA. In the present study we examined residues in BuIA that determine β subunit interaction. We mutated toxin residues and applied

double-mutant cycle analysis to investigate pair-wise interaction between toxin and receptor. Our results indicate that Pro6 of α-conotoxin BuIA interacts with residue 59 of the β subunit. Our results further indicate that this interaction may be exploited in order to create selective ligands for β4-containing nAChRs.

Materials and methods

Chemical synthesis

α-Conotoxin BuIA and toxin's analogs were synthesized on an amide resin using Fmoc chemistry and standard side protection, except on cysteine residues. Cys residues were protected in pairs with either S-trityl on Cys2 and Cys8, or S-acetamidomethyl on Cys3 and Cys13. The peptide was removed from the resin and precipitated. A two-step oxidation protocol was used to selectively fold the peptides as described previously (19).

Receptors mutagenesis

Point mutations were introduced into β2 and β4 subunits using a QuickChange site-directed mutagenesis kit (Stratagene). The receptors were in pGEMHE, pSP64, pSP65 or pBlueScript SK(-) vectors. The clones for rat α3 in pSP64 vector, β2 in pSP65 vector and rat β4 in pBS SK(-) vector were provided by S. Heinemann (Salk Institute, San Diego, CA, USA). The clones for rat β2 and rat β4 receptors in the pGEMHE vector were provided by Chuck Luetje (University of Miami, Miami, FL, USA).

All mutations were confirmed by sequencing. The notation for point mutants is to list the naturally occurring residue, its position, and residue to which it is changed. For example, β4K59T is a β4 subunit where lysine at 59 position is changed to threonine.

Electrophysiology

Capped cRNA for injection into oocytes was prepared from linearized plasmid cDNA using the mMessage mMachine kit (Ambion, Austin, TX). cRNA was purified using Qiagen RNeasy kit (Qiagen, Valencia, CA). Oocytes were prepared as described previously (15). Fifty nl of cRNA (150 ng/μl of each subunit) was injected into individual *Xenopus* oocytes. Injected oocytes were kept at 17°C in ND96 supplemented with antibiotics. All recordings were made 1-7 days after injection.

An injected oocyte was placed in a 30 μl recording chamber fabricated from Sylgard, and gravity-perfused with ND96 (96.0 mM NaCl, 2.0 mM KCl, 1.8 mM $CaCl_2$, 1.0 mM $MgCl_2$, 5 mM HEPES, pH 7.1-7.5) containing 1μM atropine (ND96A) at a rate of 2 ml/min as previously described (15). All solutions also contained 0.1 mg/mL of bovine serum albumin to reduce nonspecific adsorption of toxin. ACh-evoked currents were recorded with a two-electrode voltage-clamp amplifier (model OC-725 B, Warner Instrument Corp., Hamden, CT). The membrane potential was clamped at -70 mV, the current signal was low pass-filtered (5 Hz cut-off) and digitized at a sampling frequency of 20 Hz.

The ACh pulse to the oocyte was applied for 1 s. This was automatically done every minute. The concentration of ACh was 100 μM for all experiments. ACh was diluted in ND96A. For the control responses the ACh pulse was preceded by perfusion with ND96A. For test responses, the oocyte was exposed to toxin, either by 5- minute static bath application or by continuous perfusion with toxin solution until equilibrium. The average of three control responses just preceding a test response was used to normalize the test response to obtain "% response." Each data point of a dose-response

curve represents the average ± SE of measured response of at least three oocytes. Dose-response curves were fit with Prism software (Graph Pad Software Inc, San Diego, CA) to the equation: % response = 100/(1+([toxin]/IC_{50})^nH), where nH is the Hill coefficient.

Double mutant cycle analysis

$$\Delta\Delta G(X,Y)=\Delta\Delta G(X) + \Delta\Delta G(Y) + \Delta\Delta Gint \quad \text{(Eq. 1.1)},$$

where $\Delta\Delta G(X)$ represents the free energy change caused by a mutation of residue X in the toxin relative to its wild type, $\Delta\Delta G(Y)$ represents the change in free energy caused by mutation of residue Y in the receptor relative to its wild type. $\Delta\Delta G(X, Y)$ represents free energy change from both mutations; $\Delta\Delta Gint$ is a coupling energy, the measure of the interactions of the two mutated components. If the two residues do not interact with each other, then $\Delta\Delta Gint$ will equal 0. If the residues interact then $\Delta\Delta Gint$ will substantially differ from 0.

$\Delta\Delta Gint$ is described in terms of equilibrium constants:

$$\Delta\Delta Gint = -RTln(\Omega) \quad \text{(Eq. 1.2)},$$

where R-gas constant, 1.986cal/K·mol; T-absolute temperature, in our case T=293K, Ω-Omega, calculated as

$$\Omega=(Kd(WtWr)\times Kd(MtMr))/(Kd(WtMr)\times(Kd(MtWr)) \quad \text{(Eq.1. 3)}$$

and IC_{50} was used as an estimate of *K*d.

Results

Design of toxin analogs

α-Conotoxins are small peptides, structurally characterized by two conserved disulfide bonds that link the first and third and the second and fourth Cys residues, forming two loops. The size of the loops in different α-conotoxins is variable; in addition the residues within each loop are hypervariable and account for subtype selectivity (11).

To identify candidate toxin residues that contribute to binding selectivity of α-conotoxin BuIA, we mutated all residues positioned within the two Cys-loops of the peptide (Table 1.1).

Ala was substituted for all residues other than Pro (or Ala). Pro6 and Pro7 constrain the structure of the peptide (20), and Ala substitution at these positions might substantially alter the structure of the peptide. We therefore mutated Pro residues to 4(R)-hydroxyproline and/or 3-(R)-hydroxyproline. 4(R)-Hydroxyproline is a naturally occurring variant of Pro found in *Conus* peptides (21).

Activity of toxin analogs on α3β2 and α3β4 nAChRs

α-Conotoxin BuIA analogs were tested for activity against α3β2 and α3β4 nAChRs heterologously expressed in *Xenopus* oocytes. Results are shown in Fig. 1.1.

The results indicate that substitution of hydroxyproline for Pro6 substantially reduced activity at α3β2 nAChRs. At 10 μM concentration BuIA[P6O] inhibited only ~11% of baseline current (n=5), whereas native peptide abolished the current at the same concentration.

Mutation of Thr5, Pro7, Val10, Leu11 and Tyr12 had more modest effects. Analogs with changes at Ser4 and Ala9 potently blocked the receptor at this

concentration. In contrast, BuIA[P6O] at the same concentration abolished activity at α3β2 nAChRs. Thus, the results indicated that Pro6 plays a dominant role in toxin interaction with the receptor. Pro in the first Cys loop is a highly conserved feature across almost all α-conotoxins consistent with a critical functional role (Table 1.2). We therefore focused attention on Pro6 as a candidate for the differences in binding kinetics for β2 vs. β4 nAChRs (18).

Interaction of toxin analogs with mutant nAChRs

To assess the interaction of Pro6 with β subunits of the nAChR, we conducted double-mutant cycle analysis (22). Due to a high degree of homology between β2 and β4 nAChR subunits (Fig. 1.2), the difference in BuIA binding kinetics are likely due to non-conserved residues between subunits. Previous work identified three residues on the β subunit as likely determinants of these BuIA binding properties (23). In the β2 subunit these residues are Thr59, Val111 and Phe119. We therefore initially mutated these three nonconserved residues in the β2 subunit to residues that occur in the homologous position of the β4 subunit (Lys59, Ile111, and Gln119) (Fig. 1.2).

Double-mutant cycle analysis may be used to identify noncovalent interactions between residues of different proteins. Determination of interaction is based on alterations in additivity of the free energy resulting from mutation in toxin or receptor compared to changes in both toxin and receptor. If a toxin and a receptor residue are interacting, then the sum of the free energy change from the single mutation will <u>not</u> equal the sum of the free energy change measured with mutation in toxin and receptor (24), see *Materials and methods* for details.

Mutant cycle analyses were applied to the toxin analogs to delineate potential pair-wise interactions with the β subunit. First, we explored the interaction between Pro6 (highly conserved among α-conotoxins) and Thr59 of the β2 subunit. Substitution of 4-hydroxyproline for Pro6 decreased the potency of the toxin for wild-type α3β2 nAChRs by almost 3000-fold. This suggested that hydrophobic interaction with Pro6 is critical for binding of the toxin to this particular receptor subtype. Such interaction was disrupted by the addition of the hydrophilic 4-hydroxyl group. In contrast, however, BuIA [P6O] had enhanced affinity for an α3β2 mutant in which Thr59 was replaced with Lys found in the homologous position of the β4 subunit. The results are shown in Fig. 1.3 and Table 1.3. The experiment revealed a coupling energy of 2.4 kcal/mol for the BuIA [P6O]-β2T59K pair, indicative of interaction.

These results prompted us to examine additional mutations in Pro6 and also to examine effects of hydroxylation of the adjacent Pro7. 3- Hydroxyproline differs from 4-hydroxyproline in that the hydroxyl group in the former is adjacent to the α-carbon. Substitution of Pro6 with the 3-hydroxyproline resulted in a coupling energy of 1.01 kcal/mol for interaction with residue 59, less than that observed with 4-hydroxyproline. We next tested an electron rich 4-(R)-fluoroproline mutation to determine whether the electronegative substituent on the 4^{th} - position in Pro influenced the nAChRs binding. The BuIA [P6-fluoro] toxin analog was 23 fold less potent on the rα3β2 nAChR. The coupling energy for BuIA[P6-fluoro]-β2T59K pair was 1.1 kcal/mol, similar in magnitude to that observed with the 3-hydroxyproline analog.

We next wished to assess interaction with the 59^{th} residue of the β subunit as found in the milieu of the β4 nAChR subunit. We therefore used a β4 mutant in which

Lys59 was substituted with the Thr found in the homologous position of the β2 nAChR subunit. The coupling energy for the BuIA [P6O]-β4K59T pair was 2.4 kcal/mol, the same as that observed for the BuIA[P6O]-β2T59K pair. Thus, BuIA Pro6 couples to the 59th residue of the β subunit in the environment of the β2 as well as the β4 nAChR subunit. We further probed interactions using the 3-hydroxyproline and 4-fluoroproline analogs of BuIA. The coupling energies for BuIA[P6O(3)]-β4K59T pair were 1.3 kcal/mol and for BuIA[P6-fluoro]-β4K59T 0.8 kcal/mol. Both of these values were significantly lower than that observed with the P6O analog, consistent with results observed for the β2 subunit and residue 59.

We then probed possible interactions of Pro6 with other residues at the conotoxin binding site: Val111 and Phe119 on β2 subunit. Coupling energies for the BuIA[P6O]-β2V111I pair as well as BuIA[P6O(3)]-β2V111I pair were 0.1 kcal/mol which indicated that there was no interaction between Pro6 and Val 111. The BuIA[P6O]-β2F119Q pair gave coupling energy of 0.77 kcal/mol, indicative of weak or no interaction. BuIA[P6O(3)]-β2F119Q and BuIA[P6-fluoro]-β2F119Q gave 0.2 kcal/mol and 0.4 kcal/mol interaction, respectively. We also examined interaction of the neighboring Pro7 with the β subunit residues. The results indicated weak or no interaction. The magnitude of interaction between each of the two mutation pairs is shown in Fig. 1.3.

The BuIA Pro6 analog has reversed nAChR subtype selectivity

Pro6 of BuIA couples to the 59th residue of the β subunit. The 59th residue of the β subunit differs between β2 and β4 subunits (Fig. 1.2). This difference potentially affords the opportunity to create ligands with altered selectivity. Indeed, wild type BuIA

is five-fold more potent for α3β2 vs. α3β4 nAChRs. In contrast, BuIA[P6O] is 160-fold more potent for α3β4 vs. α3β2 nAChRs (Fig. 1.4). Thus, there is a relative shift in potency of 800-fold.

Thr/Lys difference in β2/β4 nAChR subunits causes increased potency and slow reversibility of BuIA analogs

Each of the Pro6 analogs was tested on wild type α3β2 and α3β2T59K where the Thr59 present in wild type β2 subunit is replaced with Lys found in the homologous position of the β4 subunit. In each instance, the Pro6 analog was substantially more potent on the α3β2T59K mutant. BuIA[P6O] was 1360-fold, BuIA[P6-fluoro] was 165-fold, BuIA[P6O(3)] was 132-fold more potent, on α3β2T59K nAChR than wild type α3β2 nAChRs (Fig. 1.5 and Table 1.3).

Previous findings suggested that β2Thr59 was a determinant of the α-conotoxin BuIA ability to kinetically discriminate between β2 and β4 containing nAChRs (23). In light of the increased potency of BuIA[Pro6] analogs for α3β2T59K, we examined the effects of Thr and Lys on the off-rates of BuIA Pro6 analogs. α-Conotoxins BuIA[P6O] and BuIA[P6-fluoro]. Each had rapid reversibility for α3β2 nAChRs. In contrast these analogs each had slower reversibility for the α3β4 nAChRs. In addition when β2Thr59 is changed to Lys, block by each of the peptides is slowly reversible. Conversely when β4Lys59 is changed to Thr, block by each of the peptides is rapidly reversed. Thus, Lys59 confers higher potency and slower reversibility to the peptides (Fig. 1.6).

Discussion

The acetylcholine binding site is located at the interface of two nAChR subunits. The nAChR α subunit sometimes referred to as the "principal" or (+) binding subunit. A binding pocket is created by α subunit residues that form loops known as A, B, and C. The β or "complementary" subunit contributes residues to loops known as D, E and F. Despite the names, it has become increasingly clear that the β subunit can have significant and even dominant effects on agonist and antagonist pharmacology. Some α-conotoxins show over four orders of magnitude of discrimination between nAChR subtypes that contain the same α but different β subunits (11,43,44). α-Conotoxin BuIA is unusual among the α-conotoxins in that it interacts with multiple nAChR subtypes but the kinetics of binding are determined by the β subunit. For a nAChR with a given α subunit, BuIA is most potent on β2-containing receptors. Surprisingly, however, the off-rate kinetics are much slower on β4-containing receptors.

In the present study, we synthesized mutants of BuIA to scan for residues that might account for the β-subunit specific interactions. Among the mutant peptides, the analog in which 4-hydroxyproline was substituted for Pro6 had a three order of magnitude reduction in activity at the α3β2 nAChR. In contrast, there was only a three-fold change in IC_{50} at the α3β4 nAChR.

Testing of the mutant peptides against mutant receptors revealed interaction of Pro6 and residue 59 of the β subunit. The Pro residues in α–conotoxin ImI and α-conotoxin PnIA have previously been implicated in binding to aromatic residues in the

(+) face of the α7 subunit (45,46). To our knowledge, this is the first demonstration of interaction of the conserved Pro with residues of the (-) face of the β subunit.

nAChR subunits are expressed throughout the nervous system with distinct, but overlapping anatomical distribution. This presents a challenge for selectively targeting a subpopulation of receptors in a given neuronal tissue. The present results indicate that the Thr59 to Lys difference between β2 and β4 subunits may be used to advantage in designing selective conotoxin ligands. Consistent with this, an analog of BuIA, BuIA[T5A;P6O] was recently shown to block nicotine-stimulated norepinephrine release in hippocampus. The same analog fails to block nicotine-stimulated dopamine release from caudate-putamen (47). The current study provides mechanistic insight into how the analog may achieve this selectivity. The substitution of hydroxyproline may prevent binding at an α6/β2 interface that mediates dopamine release, while sparing interaction at the nAChR α6/β4 interface that evokes norepinephrine release (18).

Table 1.1

BuIA analogs

Toxin name	Toxin structure
BuIA	G**C**STPP**CC**AVLY**C***
BuIA[S4A]	G**C**<u>**A**</u>TPP**CC**AVLY**C***
BuIA[T5A]	G**C**S<u>**A**</u>PP**CC**AVLY**C***
BuIA[P6O][1]	G**C**ST<u>**O**</u>P**CC**AVLY**C***
BuIA[P6O(3)][2]	G**C**ST<u>**O**</u>P**CC**AVLY**C***
BuIA[P6-fluoro][3]	G**C**ST<u>**P-f**</u>P**CC**AVLY**C***
BuIA[P7O]	G**C**STP<u>**O**</u>**CC**AVLY**C***
BuIA[A9S]	G**C**STPP**CC**<u>**S**</u>VLY**C***
BuIA[V10A]	G**C**STPP**CC**A<u>**A**</u>LY**C***
BuIA[L11A]	G**C**STPP**CC**AV<u>**A**</u>Y**C***
BuIA[Y12A]	G**C**STPP**CC**AVL<u>**A**</u>**C***

The sequences of all toxin analogs used in the study are shown. The mutated residues are bold and underlined.
[1]-Proline – 4(R)-hydroxyproline mutation;
[2]- Proline – 3(R)-hydroxyproline mutation,
[3]- Proline – 4(R)-fluoroproline mutation,
* -amidated C-terminus.

Table 1.2

Selected α-conotoxin sequences demonstrate a highly conserved proline residue in the first intercysteine loop.

Peptide	Sequence	Species	Reference
4/7 family of α-conotoxins			
AnIA	**CC**SH**P**A**C**AANNQDY**C***	*C. anemone*	(25)
AnIB	GG**CCS**H**P**A**C**AANNQDY**C***	*C. anemone*	(25)
AnIC	GG**CCS**H**P**A**C**FASNPDY**C***	*C. anemone*	(25)
AuIA	G**CCS**Y**P**P**C**FATNSDY**C***	*C. aulicus*	(26)
AuIC	G**CCS**Y**P**P**C**FATNSGY**C***	*C. aulicus*	(31)
EI	RDO**CC**YH**P**T**C**NMSNPQI**C***	*C. ermineus*	(27)
EpI	G**CCS**D**P**R**C**NMNNPDY**C***	*C. episcopatus*	(28)
GIC	G**CCS**H**P**A**C**AGNNQHI**C***	*C. geographus*	(29)
GID	IRDγ**CCS**N**P**A**C**RVNNOHV**C**	*C. geographus*	(30)
MII	G**CCS**N**P**V**C**HLEHSNL**C***	*C. magus*	(15)
OmIA	G**CCS**H**P**A**C**NVNNPHI**C**G*	*C. omaria*	(31)
PeIA	G**CCS**H**P**A**C**SVNHPEL**C***	*C. pergrandis*	(32)
PIA	RDP**CCS**N**P**V**C**TVHNPQI**C***	*C. purpurascens*	(33)
PnIA	G**CCS**L**P**P**C**AANNPDY**C***	*C. pennaceus*	(34)
PnIB	G**CCS**L**P**P**C**ALSNPDY**C***	*C. pennaceus*	(34)
SrIA	RT**CCS**R**O**T**C**RMγYPγL**C**G*	*C. spurius*	(35)
SrIB	RT**CCS**ROTCRMEYPγL**C**G*	*C. spurius*	(35)
Vc1.1	G**CCS**D**O**R**C**NYDHPγI**C***	*C. victoriae*	(36)
Lp1.1	G**CC**ARAA**C**AGIHQEL**C***	*C. leopardus*	(37)
4/6 family of α-conotoxins			
AuIB	G**CC**SY**P**P**C**FATNPD**C***	*C. aulicus*	(26)
4/5 family of α-conotoxins			
Ca1.1	QN**CC**SI**P**S**C**WEKYK**C**S	*C. caracteristicus*	(38)
4/4 family of α-conotoxins			
BuIA	G**CC**ST**P**P**C**AVLY**C***	*C. bullatus*	(18)
PIB	ZSOG**CC**WN**P**A**C**VKNR**C***	*C. purpurascens*	(39)
4/3 family of α-conotoxins			
ImI	G**CC**SD**P**R**C**AWR**C***	*C. imperialis*	(13)
ImII	A**CC**SDRR**C**RWR**C**	*C. imperialis*	(40)
RgIA	G**CC**SD**P**R**C**RYR**C**R	*C. regius*	(17)

Table 1.2 continued

Peptide	Sequence	Species	Reference
3/5 family of α-conotoxins			
CnIA	GR**CC**HP**C**GKYYS**C***	*C. consors*	(41)
GI	E**CC**NP**C**GRHYS**C***	*C. geographus*	(42)
GIA	E**CC**NP**C**GRHYS**C**GK*	*C. geographus*	(42)
GII	E**CC**NP**C**GKHFS**C***	*C. geographus*	(42)
MI	GR**CC**HP**C**GKNYS**C***	*C. magus*	(14)

Conserved cysteine residues are highlighted in bold-face. Conserved proline is highlighted in red and shaded. For post-translational modifications: γ, γ-carboxyglutamate; Z, pyroglutamic acid; O, hydroxyproline; *, amidated C-terminus, Y, Sulfotyrosine.

Table 1.3

IC_{50}s and calculated coupling energies.

Receptor	Toxin	IC_{50}	95% CI for IC_{50}	Ω or 1/Ω	ΔGint, kcal/mol, absolute value
WT(α3β2)	BuIA[1]	5.7 nM	4.6-7.2 nM		
WT(α3β2)	BuIA [P6O]	15 μM	12-19 μM		
WT(α3β2)	BuIA [P6-fluoro]	130 nM	81-210 nM		
WT(α3β2)	BuIA [P6O(3)]	5.4 μM	3.0-10 μM		
WT(α3β2)	BuIA [P7O]	81 nM	70-94 nM		
α3β2T59K	BuIA[1]	0.24 nM	0.19-0.32 nM		
α3β2T59K	BuIA [P6O]	11 nM	7.0-17 nM	60	2.4
α3β2T59K	BuIA [P6-fluoro]	0.79 nM	0.58-1.1nM	7.0	1.1
α3β2T59K	BuIA [P6O(3)]	41 nM	28-59 nM	5.5	1.0
α3β2T59K	BuIA [P7O]	1.2 nM	0.9-1.6 nM	2.8	0.61
α3β2V111I	BuIA[1]	9.0 nM	7.6-11 nM		
α3β2V111I	BuIA [P6O]	20 μM	15-26 μM	1.2	0.12
α3β2V111I	BuIA [P6-fluoro]	2.6 μM	2.5-2.7 μM	12	1.5
α3β2V111I	BuIA [P6O(3)]	10 μM	7.9-13 μM	1.2	0.11
α3β2V111I	BuIA [P7O]	970 nM	540-1700 nM	7.6	1.2
α3β2F119Q	BuIA[1]	0.74 nM	0.59-0.91 nM		
α3β2F119Q	BuIA [P6O]	530 nM	400-700 nM	3.8	0.77
α3β2F119Q	BuIA [P6-fluoro]	36 nM	30-43 nM	2.1	0.44
α3β2F119Q	BuIA [P6O(3)]	1.0 μM	0.83-1.2 μM	1.4	0.21
α3β2F119Q	BuIA [P7O]	20 nM	16-24 nM	1.9	0.37
WT(α3β4)	BuIA[1]	28 nM	22-35 nM		

Table 1.3 continued

Receptor	Toxin	IC_{50}	95% CI for IC_{50}	Ω or 1/Ω	ΔGint, kcal/mol, absolute value
WT(α3β4)	BuIA [P6O]	94 nM	84-100 nM		
WT(α3β4)	BuIA [P6-fluoro]	81 nM	60-110 nM		
WT(α3β4)	BuIA [P6O(3)]	510 nM	400-640 nM		
WT(α3β4)	BuIA [P7O]	11 nM	9.6-13 nM		
α3β4K59T	BuIA	34 nM	29-38 nM		
α3β4K59T	BuIA [P6O]	6.6 μM	4.2-9.0 μM	58	2.4
α3β4K59T	BuIA [P6-fluoro]	410 nM	340-490 nM	4.2	0.84
α3β4K59T	BuIA [P6O(3)]	5.9 μM	4.8-7.4 μM	9.7	1.3
α3β4K59T	BuIA [P7O]	135 nM	88-210 nM	10	1.3

Coupling energies were calculated using Eq.2 (see *Materials and methods*).
[1]- Values are from ref *23*.

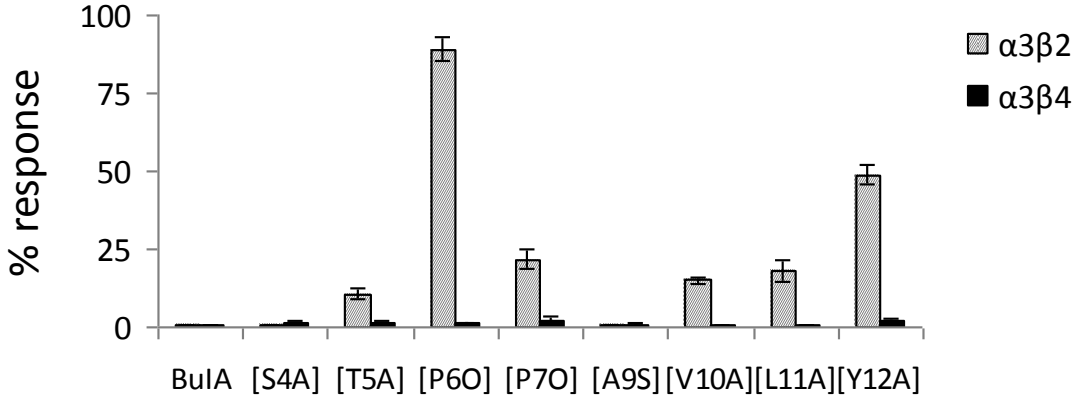

Figure 1.1 Mutations in α-conotoxin BuIA differentially affect α3β2 vs. α3β4 nAChRs. The noncysteine residues of α-conotoxin BuIA were mutated to alanine (A) or hydroxyproline (O) and tested on rat α3β2 and α3β4 nicotinic receptors heterologously expressed *in Xenopus* oocytes as described in *Materials and methods.* Error bars are S.E.M., n= 3-6 for each condition.

```
                                                                                •
rat β4              ANAEEKLMDDLLNKTRYNNLIRPATSSSQLISIRLELSLSQLISVNEREQIMTTSIWLKQ 60
human β4            ANAEEKLMDDLLNKTRYNNLIRPATSSSQLISIKLQLSLAQLISVNEREQIMTTNVWLKQ 60
rat β2              TDTEERLVEHLLDPSRYNKLIRPATNGSELVTVQLMVSLAQLISVHEREQIMTTNVWLTQ 60
human β2            TDTEERLVEHLLDPSRYNKLIRPATNGSELVTVQLMVSLAQLISVHEREQIMTTNVWLTQ 60

                                                                  *       *
rat β4              EWTDYRLAWNSSCYEGVNILRIPAKRVWLPDIVLYNNADGTYEVSVYTNVIVRSNGSIQW 120
human β4            EWTDYRLTWNSSRYEGVNILRIPAKRIWLPDIVLYNNADGTYEVSVYTNLIVRSNGSVLW 120
rat β2              EWEDYRLTWKPEDFDNMKKVRLPSKHIWLPDVVLYNNADGMYEVSFYSNAVVSYDGSIFW 120
human β2            EWEDYRLTWKPEEFDNMKKVRLPSKHIWLPDVVLYNNADGMYEVSFYSNAVVSYDGSIFW 120

rat β4              LPPAIYKSACKIEVKHFPFDQQNCTLKFRSWTYDHTEIDMVLKSPTAIMDDFTPSGEWDI 180
human β4            LPPAIYKSACKIEVKYFPFDQQNCTLKFRSWTYDHTEIDMVLMTPTASMDDFTPSGEWDI 180
rat β2              LPPAIYKSACKIEVKHFPFDQQNCTMKFRSWTYDRTEIDLVLKSDVASLDDFTPSGEWDI 180
human β2            LPPAIYKSACKIEVKHFPFDQQNCTMKFRSWTYDRTEIDLVLKSEVASLDDFTPSGEWDI 180
```

Figure 1.2 Sequence alignment of rat and human β2 and β4 nAChR subunits. The nonconserved residues of the complementary binding site, important for α-conotoxin binding, are indicated.

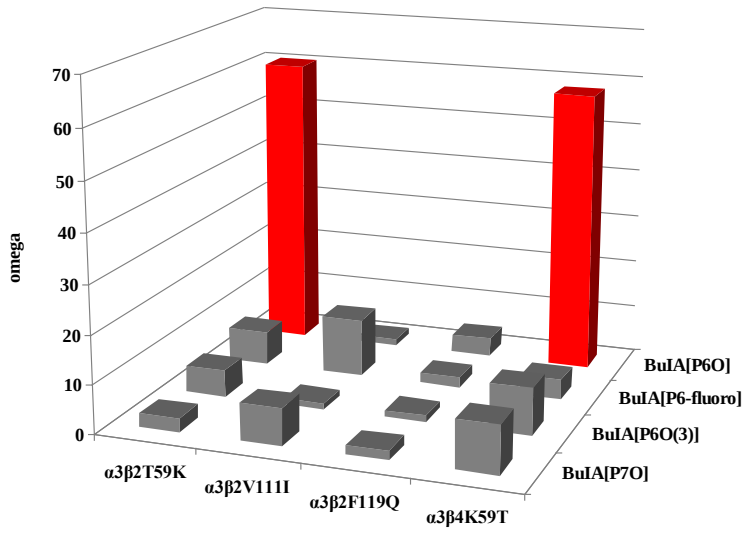

Figure 1.3 Coupling coefficient values for toxin-receptor mutant pairs. Wild type and mutant peptides were tested on wild type and mutant receptors heterologously expressed in *Xenopus* oocytes. The coupling coefficient, Ω, for the magnitude of interaction was calculated as described in *Materials and methods*. Absolute values were used and are shown in Table 1.3.

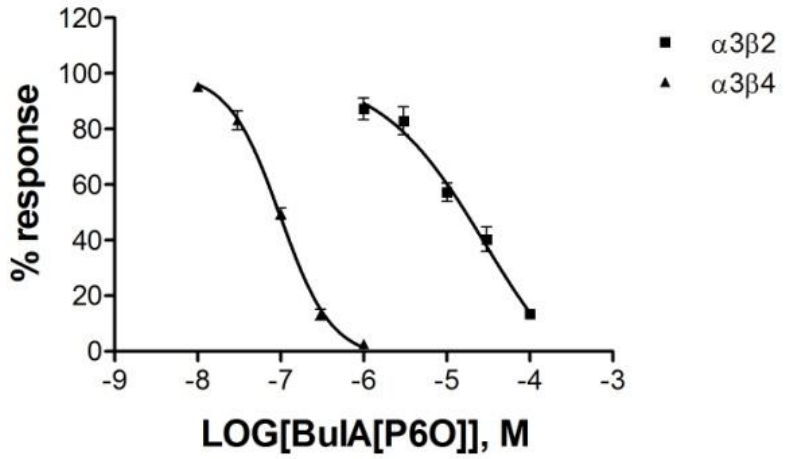

Figure 1.4 Concentration-response curves for BuIA[P6O] on rα3β2 and rα3β4 nAChRs. Substitution 4-*trans*-hydroxyproline for Pro6 enables the peptide to selectively block α3β4 vs. α3β2 nAChRs.

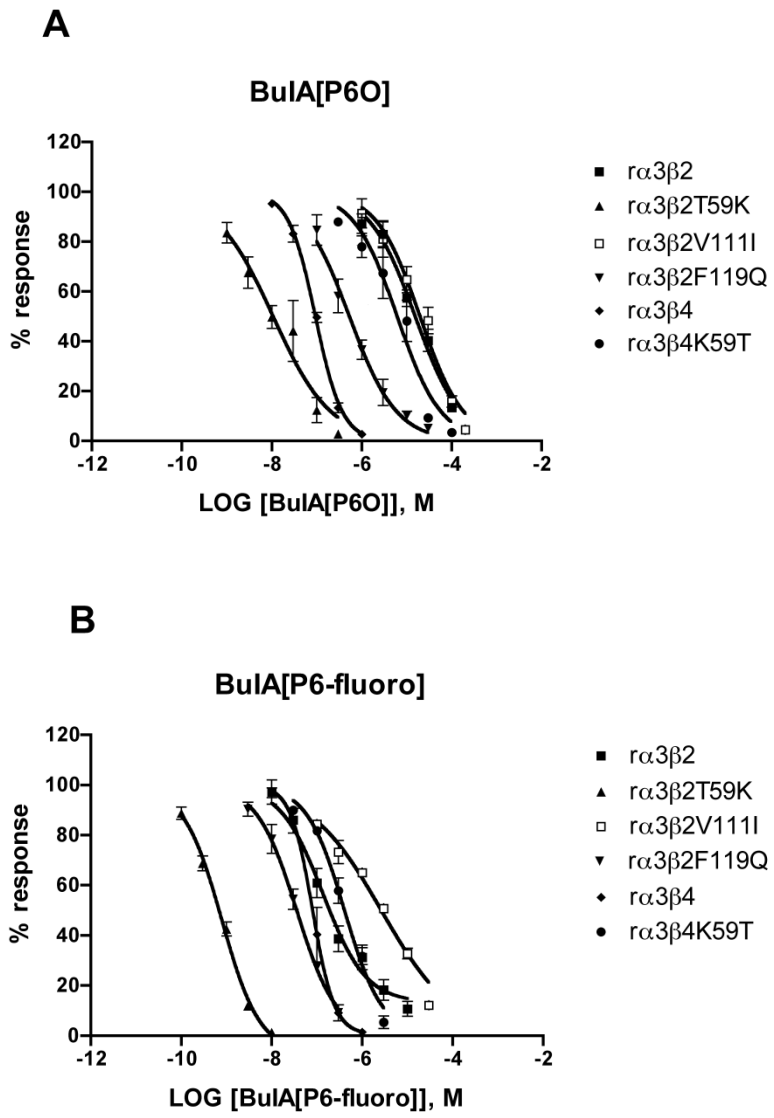

Figure 1.5 Concentration-response of toxin analogs tested on receptor mutants. Concentration-response analysis indicates that Lys59 of the β4 subunit favors toxin binding. A, BuIA[P6O], B, BuIA[P6O(3)], C, BuIA[P6-fluoro], and D, BuIA[P7O] show higher affinity for the rα3β2T59K receptor variant compared to wild type rα3β2 nAChR. BuIA[P6O] is 1360-fold, BuIA[P6-fluoro] is 165-fold, BuIA[P6O(3)] is 132-fold and BuIA[P7O] is 67-fold more potent on rα3β2T59K compared to rα3β2. Error bars are S.E.M. Values are shown in Table 1.3, n=3-11.

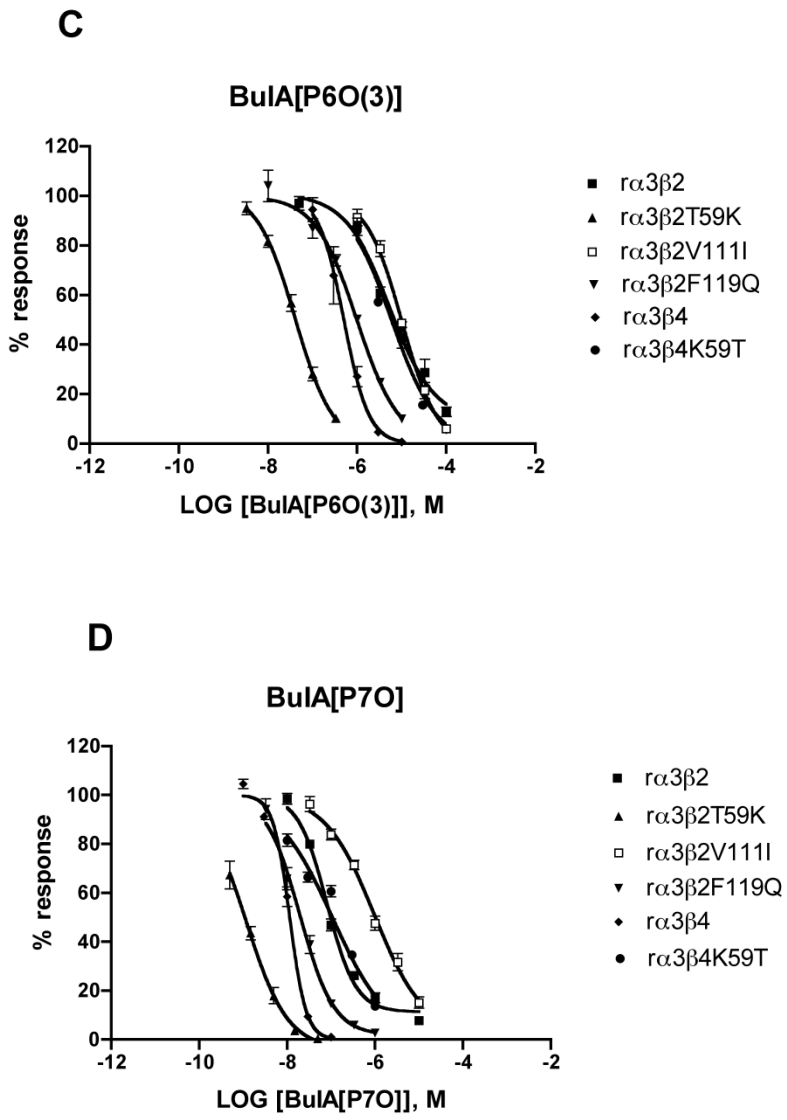

Figure 1.5 Continued

Figure 1.6 Position 59 of the β subunit alters kinetics of toxin unblock. Rat nAChRs were expressed in *Xenopus* oocytes as described in *Experimental Procedures*. A control response (C) to ACh was measured. Following a 5-minute toxin application, ACh was again applied followed by toxin wash-out. Recovery from toxin block was measured at 1-minute intervals. BuIA[P6O] was applied as indicated to (A) w.t. rat α3β2 nAChRs; (B) w.t. α3β4 nAChRs; (C) a point mutant of α3β2 where Lys59 found in the w.t. β4 subunit was substituted for Thr59 found in the w.t. β2 subunit; and (D), a point mutant of α3β4 where Thr59 found in the w.t. β2 subunit was substituted for Lys59 found in the w.t. β4 subunit. Note in each instance that recovery from toxin block is slower when position 59 of the β subunit is Lys. Likewise, BuIA[P6-fluoro] was applied as indicated to (E) w.t. rat α3β2 nAChRs; (F) w.t. α3β4 nAChRs; (G) a point mutant of α3β2 where Lys59 found in the w.t. β4 subunit is substituted for Thr59 found in the w.t. β2 subunit; and (H), a point mutant of α3β4 where Thr59 found in the w.t. β2 subunit is substituted for Lys59 found in the w.t. β4 subunit. Note again that recovery from toxin block is slower when position 59 of the β subunit is Lys.

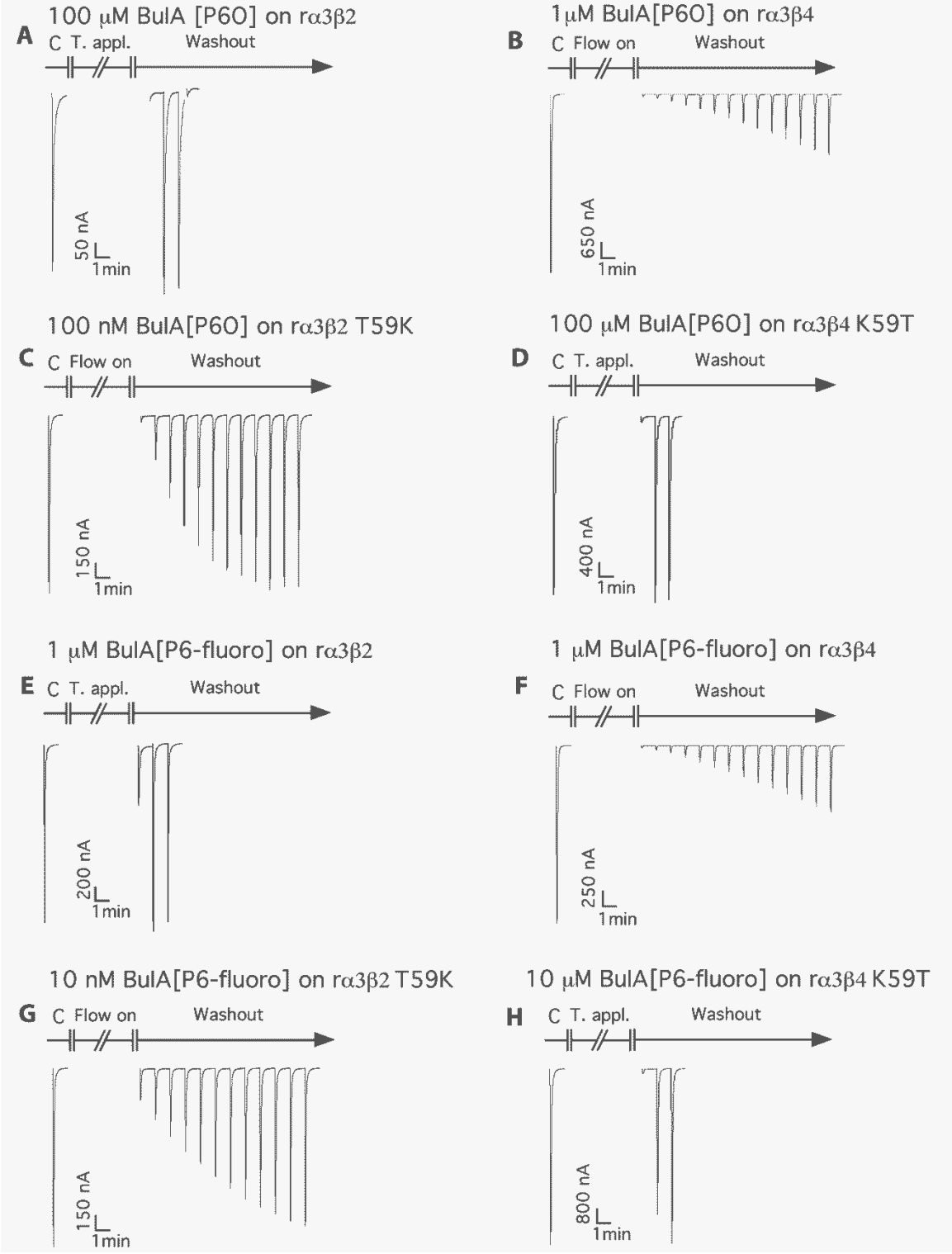
A
100 μM BulA [P6O] on rα3β2
C T. appl.
Washout
50 nA
1min
B
1μM BulA[P6O] on rα3β4
C Flow on
Washout
650 nA
1min
C
100 nM BulA[P6O] on rα3β2 T59K
C Flow on
Washout
150 nA
1min
D
100 μM BulA[P6O] on rα3β4 K59T
C T. appl.
Washout
400 nA
1min
E
1 μM BulA[P6-fluoro] on rα3β2
C T. appl.
Washout
200 nA
1min
F
1 μM BulA[P6-fluoro] on rα3β4
C Flow on
Washout
250 nA
1min
G
10 nM BulA[P6-fluoro] on rα3β2 T59K
C Flow on
Washout
150 nA
1min
H
10 μM BulA[P6-fluoro] on rα3β4 K59T
C T. appl.
Washout
800 nA
1min

CHAPTER 2

5’ UNTRANSLATED REGION OF HUMAN α9 SUBUNIT IS CRITICAL TO HETEROLOGOUS EXPRESSION OF α9* NICOTINIC ACETYLCHOLINE RECEPTORS

Introduction

Nicotinic acetylcholine receptors (nAChRs) are ACh-gated ion channels implicated in many physiological as well as pathophysiological processes. The role of nAChRs in mediating EPSPs at synapses in autonomic ganglia (48,49) and at the skeletal neuromuscular junction is well established (50,51). In the CNS, nAChRs are involved in modulation of neurotransmitter release (52) and in attention and memory (53,54). The pathological conditions where involvement of nAChRs have been implicated include Alzheimer's and Parkinson's diseases (55,56), nicotine addiction (57,58) and schizophrenia (59,60). Seventeen vertebrate nAChR subunits have been cloned to date (α1 through α10, β1 through β4, γ, δ, and ε) (61). The nAChR is formed from five subunits, either homomeric receptors (α7, α9) containing five identical subunits or heteromeric receptors (for example, α4β2, α3α5β4, α6α4β2β3, or α9α10).

α9-containing nAChRs are unique among neuronal nAChRs in that they are found mainly outside of the CNS (62-66). Also, unlike other nAChRs, they are inhibited by nicotine (62,67,68). α9-containing nAChRs play roles in pain (69-74), inflammation, keratinocyte adhesion (75), and in mediating synaptic transmission between the efferent olivocochlear fibers and cochlear hair cells (76,77).

With advances in molecular biology, it became possible to isolate and sequence the genes encoding nAChRs. α9 and α10 subunits were among the last nicotinic receptor subunits to be isolated and characterized. The clone encoding the α9 subunit was originally obtained from a rat olfactory epithelium cDNA library (62). *X. laevis* oocytes injected solely with rat α9 cRNA yielded homomeric receptors that responded to 100 μM ACh with currents that ranged from 20 to 500 nA (62). The clone encoding the rat α10

subunit was isolated from an adult rat cochlea cDNA library (78). The coinjection of rat α9 and rat α10 cRNAs into oocytes resulted in oocytes with ~ 100-fold larger ACh-gated currents (I_{ACh}) than oocytes injected solely with α9 cRNA. Subsequently, the sequences of human α9 and α10 subunits were determined from keratinocytes (75) and inner-ear neuroepithelium (79), respectively.

To study the pharmacological properties of nAChRs, heterologous expression systems are often used. Mammalian cell lines such as HEK293 and SH-EP1 cells are frequently used to characterize nAChRs (80,81). Besides mammalian cells, oocytes of *Xenopus laevis*, the African clawed frog, have been frequently used for heterologous expression. These oocytes provide several advantages for the study of receptors. They are large and thus easy to handle and to inject with RNA, have long life-times (several days) and can be maintained under relatively simple culture conditions. Oocytes are largely free of endogenous receptors that could interfere with the signals of exogenously expressed channels/receptors. Thus, oocytes have been extensively used to characterize the biophysical and pharmacological properties of nAChRs. They have also been used to study the stoichiometry of receptor subunits, the contribution of different subunits to the properties of receptors, and the structure-function relationships with various ligands. For most nAChRs, oocytes have worked extremely well as an expression host (82-84). However, in some instances cRNA-injected oocytes have failed to yield readily detectable I_{ACh}. For instance, human α9 cRNA-injected oocytes have only small I_{ACh} compared to oocytes injected with its rat counterpart (85,86). There is no report to date of successful functional expression of human α9-containing receptors in mammalian cell lines and few reports of successful transfection of rat a9-containing receptors (87,88).

The translational efficiency of nAChRs in oocytes is influenced by the structure of the injected cRNA (89,90) including the Kozak sequence (91), the secondary structure (92,93) and composition of untranslated regions (94,95). The 5' leader sequence preceding the coding region plays an important role in the binding of cap-binding proteins and in facilitation of translation initiation (96). One approach to improve the translation in oocytes is to flank the gene-encoding sequence with the untranslated regions of highly translatable proteins of *X. laevis*, such as β-globin (97,98). When 5' and 3'untranslated regions (UTRs) of human interferon-β mRNA are replaced by those of *X. laevis* β-globin mRNA, the translation is increased as much as 20- and 300- fold in reticulocyte lysates and in *X. laevis* oocytes, respectively (99). The *X. laevis* β-globin leader sequence exerts its facilitatory effect presumably by increasing translation initiation, and not by increasing the binding of limiting factors (97). However, for human α9, the addition of the *X. laevis* β-globin sequence to the 5' and 3' UTRs is not sufficient to produce high expression levels.

In this report, we show that the human α9 subunit is the limiting factor in the expression of human α9α10 nAChRs in *X. laevis* oocytes. Furthermore, we found that this expression can be substantially improved by the insertion of the 5' leader sequence of alfalfa mosaic virus RNA4 (AMV) to the human α9 5' UTR.

Materials and methods

cDNA constructs

cDNAs encoding α9 and α10 nAChR subunits from rat were provided by A. B. Elgoyhen (University of Buenos Aires, Argentina). The rat α9 cDNA was in a pGEMHE (98) vector between SmaI and EcoRI restriction sites, and the rat α10 cDNA was in a

pSGEM vector (a modified pGEMHE vector) between EcoRI and XhoI restriction sites. cDNAs encoding human α9 and human α10 subunits, in the pGEM-11Zf(+) vector, were generously provided by L. Lustig (University of California San Francisco, San Francisco, CA). The cDNAs encoding human subunits were subsequently inserted into the pSGEM vector between EcoRI and XhoI restriction sites. The oligonucleotides encoding the 5'leader sequence of alfalfa mosaic virus RNA4 (AMV) were synthesized at the University of Utah core facility. The sequence of the synthesized oligonucleotides was as follows: sense- 5' GGGTTTTTATTTTTAATTTTCTTTCAAATACTTCCACCG 3'; antisense-

5' AATTCGGTGGAAGTATTTGAAAGAAAATTAAAAATAAAAACCCGC 3'. The oligonucleotides were diluted in 10 mM Tris-Cl, pH 8.5 to a final concentration of 107 μM for sense oligonucleotide and 80 μM for antisense oligonucleotide. 20 μL of each oligonucleotide was mixed in an annealing reaction tube. The annealing reaction was as follows: exposure to 95 °C for 10 minutes followed by cooling to 25 °C over a period of 45 minutes. The annealed oligonucleotide was ligated into MCS of pSGEM vector between the SacII and EcoRI restriction sites.

cRNA synthesis

The NheI enzyme was used to linearize the vector encoding human α9 and human α10 subunits. *In vitro* transcription was performed using the mMessage mMachine T7 kit (Ambion, Austin, TX). The reaction was followed by DNase treatment. The cRNA was purified with a Qiagen RNeasy kit (Qiagen, Valencia, CA, USA). The cRNA concentration was determined by measuring absorbance at 260 nm on an Epoch spectrophotometer.

Oocyte isolation and injection

The isolation of the oocytes was performed as previously described (15). Briefly, stage IV-V oocytes were isolated from anesthetized adult frog. The oocytes were kept at 17° C in ND96 (96 mM NaCl, 1.8 mM $CaCl_2$, 2.0 mM KCl, 1.0 mM $MgCl_2$, 5mM HEPES, pH 7.1-7.5) supplemented with antibiotics (50 U/mL penicillin, 50 μg/mL streptomycin, 50 μg/mL gentamicin). The oocytes were injected with 50.6 nL of cRNA and incubated for 1-3 days before recording. The amount of cRNA injected into each oocyte varied in different experiments: to compare level of expression of human and rat α9α10 receptors, 3.3 ng/oocyte of each subunit cRNA was injected. To compare the level of expression of human receptors formed from subunits injected at different ratios, 4.4 ng cRNA of each nAChR subunit was injected into individual oocytes when a ratio of (1) is indicated and 22 ng cRNA was injected when a ratio of (5) is indicated. For all other experiments, 14.4 - 32 ng/oocyte of cRNA was injected.

Two-electrode voltage clamp recording

ACh-gated currents were recorded from oocytes as previously described (15). Briefly, an oocyte was placed in ~30 μL chamber (4mm diameter X 2mm deep) fabricated from Sylgard and gravity-perfused with ND96 at a constant flow rate (~2 mL/min). The oocyte's membrane potential was held at -70 mV using an OC-725B two-electrode voltage clamp amplifier (Warner Instrument Corp., Hamden, CT). To evoke I_{ACh}, the perfusion of ND96 was replaced for 1 second with ND96 containing100 μM ACh; such a pulse of ACh was applied once per minute. The peak of the ACh-gated current (I_{ACh}) was measured and the average of six consecutive I_{ACh} responses served as the control current response.

To minimize potential batch-to-batch variability, oocytes from the same isolation were used to compare the expression of receptors formed from unmodified and modified nAChR subunits. Furthermore, all recordings for a given comparison were performed on the same day.

Data analysis

Data are expressed as mean ± SEM. Statistical comparisons between two groups were done using Student's t-tests, and those between multiple groups were done using ANOVA test with Tukey's post-hoc comparison.

Results

Human α9α10 nAChRs express poorly in X. laevis oocytes

Previous investigations of human and rat α9-containing receptors reported difficulties in the expression of human α9-containing receptors (85,86). Consistent with these reports, when cRNAs encoding human α9 and human α10 subunits of nAChRs were co-injected into oocytes at a 1:1 molar ratio, 100 μM ACh produced small currents (Fig. 2.1A top), which on average were 30 ± 3 nA (Fig. 2.1B). Currents of this low magnitude are difficult to utilize for medium throughput pharmacological testing. In contrast, co-injection of rat α9 and rat α10 subunits yielded large currents (Fig. 2.1A bottom) with an average amplitude of 8067 ± 1638 nA (Fig. 2.1B). The difference in functional expression between rat α9α10 and human α9α10 nAChRs might be due to the inefficient translation of the human α9 or human α10 subunit or both, and this was explored in experiments described below.

Functional expression of α9 versus α10 subunits

In order to assess the influence of α9 *vs*. α10 subunits on the functional expression of α9α10 nAChRs, we injected cRNA encoding subunits from different species (i.e., rat *versus* human) at a 1:1 ratio. When human α9 was co-expressed with rat α10, the current amplitude was invariably low in all three batches of oocytes tested, averaging from 5 ± 1 nA to 50 ± 15 nA (Fig. 2.2 and Table 2.1). When rat α9 was co-expressed with human α10, the current was readily detectable (Fig. 2.2 and Table 2.1) and at a level similar to that seen after co-injection of rat α9 with rat α10 subunits (Fig. 2.1A bottom and Fig. 2.1B); the average current amplitude ranged between 732 ± 155 nA and 9755 ± 596 nA, depending on which of three batches of oocytes was used. There are at least two possible reasons for the low functional expression: A) rat α10 co-expressed with human α9 produced functionally impaired receptors or B) human α9 subunits are not translated efficiently in oocytes.

Inefficient translation of the human α9 subunit

appears to limit assembly of functiona

l human α9/human α10 receptors

When cRNAs encoding human α9 and human α10 subunits were co-injected at a 1:1 ratio, the I_{ACh} rarely reached 1 μA with the average response equal to 142 ± 23 nA. Oocytes injected with a 5:1 ratio had currents averaging 5171 ± 748 nA. Injections at a 1:5 ratio produced oocytes with low average I_{ACh} amplitude equal to 6.5 ± 3.9 nA (Fig. 2.3 and Table 2.2). Thus, more abundant cRNA for the α9 subunit leads to substantially enhanced functional expression of α9α10 nAChRs. This increased functional expression

suggests that translation of the human α9 subunit is likely a limiting factor in the assembly of α9α10 receptors.

AMV insertion and expression of human α9-containing nAChRs

Previous investigators have shown that incorporation of 5'UTR of the *Xenopus laevis* β-globin gene facilitates the *in vitro* translation of different proteins in oocytes and other expression systems (97,98,100). In pGEMHE and pSGEM vectors the 5' leader sequence of the receptor subunit includes the 5'UTR of *X. laevis* β-globin, restriction sites of the vector's multiple cloning site, and the native 5'UTR of the subunit.

Plant viruses use host translational machinery for replication. RNAs of many plant viruses possess efficient translation enhancers (101) that can be used in order to improve the translation of recombinant proteins or expression of receptors in heterologous systems. Among such enhancers are untranslated regions from different viral RNAs. The 5'UTR from alfalfa mosaic virus RNA4, the 3'UTR of brome mosaic virus and the 5'leader of tobacco mosaic virus were shown to be able to enhance the mRNA translation of foreign proteins (102-106).

In an attempt to improve the translation of human α9/α10 we modified the 5'leader sequence of human α9 and human α10 subunits by introducing the 5'UTR of RNA4 of alfalfa mosaic virus (AMV) into the multiple cloning site of the pSGEM vector (Fig. 2.4B) between SacII and EcoRI sites, after the 5'UTR of β-globin and in front of the nAChR subunit.

The AMV incorporation improved the functional expression of human α9 homomeric receptors by 37- to 101-fold, and the human α9α10 heteromeric receptors by 41- to 250-fold, depending on the batch of oocytes used (Fig. 2.5 and Tables 2.3 and 2.4).

Despite the variability in the expression levels of human α9 and α9α10 receptors, which is also commonly observed for other nAChRs, the large improvement in expression was highly reproducible.

Discussion

In this study, we determined that the functional expression of human α9 subunits of nAChRs in *X. laevis* oocytes depended on the composition of its 5'untranslated region. By introducing the 5' leader sequence of alfalfa mosaic virus RNA4 into the multiple cloning site of the pSGEM vector just preceding the coding region of human α9 or α10 subunits, we created a vector that gave ~ 70-fold higher expression levels of α9 homomeric receptors and ~ 80-fold higher expression levels of α9α10 heteromeric receptors compared to those achieved with unmodified vectors.

Since the early demonstration that mRNA encoding nicotinic receptors from *Torpedo californicus* electric organ could produce functional receptors when it is injected into oocytes of *X. laevis* (107,108), oocytes have frequently been used as an exogenous expression system to study the pharmacology of nAChRs. In most cases, the receptor subunits assemble into functional receptors (83,109,110). However, sometimes the cRNA injected into oocytes fails to yield functional receptors. For example, when cRNA encoding the α6 subunit is co-injected with cRNA encoding the β2 or β4 subunit, there is little or no detectable ACh-gated current (111). In our laboratory, the unmodified cRNA of human α9 nAChRs failed to produce functional receptors. Other authors also reported difficulties in expressing human α9-containing nAChRs (85,86). The ability of cRNAs of rat α9 and human α10 subunits, but not those of human α9 and rat α10, to form receptors

with high levels of functional expression suggests that human α9 is a limiting factor in the assembly of functional receptors.

There are several possible factors that can influence the level of functional expression of nAChRs in the *X. laevis* oocyte system. First, the cRNA composition might prevent or interfere with efficient translation. For example, formation of secondary structures may take place that prevent efficient binding of cap-binding proteins and initiation of translation (91). The nucleotide sequence just preceding the start codon is important for translation initiation. In eukaryotes, the optimal sequence surrounding the start codon is GCCA/GCCaugG (112). If the purine at the -3 position is changed to a pyrimidine, the efficiency of translation initiation might be reduced. Second, a high G+C content of mRNA can halt efficient transcription and translation by formation of secondary structures. For example, the gene encoding human acetylcholinesterase (AChE) is highly G+C rich (65%) which results in the formation of a secondary structure in the 5'region (113) that serves as an attenuator of transcription. In addition, two highly homologous and highly G+C-rich genes encoding *Bungarus* and rat acetylcholinesterases have strikingly different rates of transcription with approximately equal translation in oocyte functional tests (114). The difference in the transcription rate is believed to be determined by the differences in the coding sequences.

The G+C content of human α9 mRNA is 49 % for the gene-coding sequence compared to 51% for rat mRNA. α10 subunits are richer in G+C content with a 65% in the human and 59% in the rat subunit. Thus the G+C content of human α9 is only slightly lower than its rat counterpart. Based on the relatively equal G+C composition of human and rat α9 mRNAs and high homology in nucleotide sequences of gene-coding sequences

it is unlikely that G+C content contributes to the low level of functional expression observed from unmodified human α9 subunit in our study.

The UTR is another factor influencing translational efficiency. It was shown to be important for the translation of different proteins in different expression systems. Mutations in the UTR affect the translation of aspartyl protease BACE1 protein and HT3A receptor (115-117). When the 5'UTR of BACE1 is present, the protein, but not mRNA, level in transfected HEK293, COS7 and H4 cells is reduced as much as 90%. The inhibitory effect of the 5'UTR is due to the upstream open reading frame (uORF) (115,117). Due to their importance, the UTR regions are frequently modified to improve translation. For example, it became a common practice to include 5'- and 3'- UTRs of *Xenopus* β-globin into expression vectors to flank the gene-coding region (98). UTRs of viruses have also been used to replace native UTRs, which results in improved yields of translated proteins or improved functional expression of receptors. For example, the 5'UTR of tobacco mosaic virus enhances the translation of chloramphenicol acetyltransferase and β-glucuronidase in tobacco mesophyll protoplasts, *E. coli*, and *Xenopus* oocytes (102,104,105,118). The facilitatory effect of the 5'leader is due to recruitment of eukaryotic initiation factor 4G indirectly via heat shock protein 101 (119).

The alfalfa mosaic virus is an RNA virus consisting of three genomic RNAs and one subgenomic RNA (RNA4). RNA1 and RNA2 encode the replicase proteins P1 and P2, whereas RNA3 encodes viral movement protein (MP). RNA4 is 881-nucleotides long, with a 661-nucleotide long coding sequence that encodes a coat protein required for infectivity and replication of the virus (120). The 5'UTR of RNA4 is 39-nucleotides long, uracil rich and was shown to be able to improve the translation of foreign proteins.

Computer-based structure prediction as well as nuclease-sensitivity analysis indicate the unstructured character of the 5'leader sequence, which can facilitate cap-independent translation initiation (121). This fact might be relevant if cap-dependent translation initiation of unmodified human α9 subunit is disrupted. The substitution of the native 5'UTR with a 37-base-pair AMV RNA4 leader was shown to improve the translation of several proteins (104,118). For example, *in vitro* translation of human interleukin 1β and barley α-amylase improved as much as 35-fold (105). Also, the introduction of AMV into the 5'leader of $GABA_A$ receptors improved the expression of those receptors in *X. laevis* oocytes (118).

The 5'UTRs of human nicotinic receptors may be an important factor for receptor function, considering evidence from other systems suggesting that this region could have the regulatory elements important for translation initiation (115,122,123). Many human nAChR subunits have upstream uATG repeats (uATGs) and upstream open reading frames (uORFs). For example, human α9 has an uORF with a length of 36 codons. uORFs are involved in translational regulation of oncogenes by suppressing the level of translation (124,125). It is believed that the uORF causes the small ribosomal subunit to stall and therefore halt translation initiation (126). How the uORF affects the translation of the α9 subunit is an open question. When cRNAs encoding nicotinic receptor subunits are injected into oocytes at a 1:1 molar ratio, it is assumed that the two subunits will be translated with equal efficiencies so the amount of protein of the two subunits will also be produced in a 1:1 ratio. However, different receptor subunits might be translated with different efficiencies.

mRNA stability might be a contributing factor to the observed different levels of expression between unmodified human α9-containing receptors and rat α9-containing receptors. One of the factors that determines the stability of mRNA is located within 3'-end of mRNA. In particular, the poly(A) tail is required to ensure high functional stability of the mRNA as was shown for rabbit globin protein (127,128). The 3'UTR of the human α9 subunit had a short (6 nucleotides) native 3'UTR, followed by the 3' UTR of *Xenopus* β-globin, followed by a poly(A) tail. In contrast, the modified construct incorporated the 5' UTR of the alfalfa mosaic virus RNA4. This addition may slow degradation of the mRNA.

Another factor that may contributes to the fast turnover of mRNA is an AU-rich region at 3'-untranslated region. Many RNA-binding proteins such as ELAV-like proteins (HuD, Hel-N1, HuC, HuR) bind to AU-rich regions at the 3'-untranslated region of RNA and prevent degradation of mRNA (129). Human α9 as well as rat α9 subunit 3'UTRs have six non-overlapping AUUUA motifs separated by non-AU nucleotides in a U-poor region. In addition, they have one AAAAUUUAAAA motif.

A second possibility for low expression level of receptors in oocytes is the lack of postrtranslational modifications in the oocyte expression system. The possible posttranslational modifications of nAChRs include proteolytic cleavage, disulfide bond formation, glycosylation, palmitoylation, fatty acid acylation, phosphorylation, amidation, hydroxyprolination, proline isomerization, etc. (130-133). The lack of functional expression of α6-containing receptors is likely due to posttranslational mechanisms, insofar as functionality is achieved when the C-terminus of the α6 subunit is replaced with the C-terminus of an α3 subunit implying that important regulatory

elements for efficient receptor function are located outside of ligand-binding domain (111).

A third possibility is the lack of appropriate chaperones in oocytes. There are several chaperones described for nicotinic receptors such as BiP, calnexin, Erp57, and RIC3 (134,135), which facilitate proper folding and improve functional expression of receptors. Nicotine exposure causes an upregulation of nicotinic AChRs in brain as well as *in vitro*, and a possible explanation of this effect is through the chaperoning by nicotine (136-138). The RIC-3 is a chaperone that upregulates the expression of α7 nAChRs in oocytes (139-142). Interestingly, RIC-3 has no effect on the expression of α9 receptors (87,143).

There are few reports of successful expression of α9 receptors in mammalian cells (144). GH4C1 cell line derived from pituitary gland was successfully transfected with rat α9α10 receptors (88). Here, the average ACh-evoked currents ranged between 16 pA to 300 pA. Also, an α9/HT3a chimera, where the N-terminus of rat α9 was fused to the C-terminus of mouse HT3a receptor, produced functional receptors (145). Mouse α9α10 receptors were successfully transfected into HEK293 cells (144). The problem of the lack of expression of human α9 receptor in mammalian cell lines was addressed in several reports (87,144-146). It was shown that co-transfection of human α9 and α10 subunit with AChR-associated proteins rapsyn and chaperone RIC-3 in CL4 cells increased the cytosolic calcium level after application of 100 μACh but no measurements of ionic current from α9-containing receptors were reported (146). It is still an open question as to whether the lack of functionality in mammalian cells is due to inefficient transcription,

translation, improper folding, and lack of chaperoning or posttranslational modifications or a combination of these.

In our current study, we observed the effect of the 5'UTR of the human α9 subunit on the expression of functional receptor. We conclude that the inefficient expression of human α9-containing receptors can be improved by modifying 5'UTR of the cRNA encoding the subunit. It is possible that the initiation codon of the original unmodified subunit is in unfavorable form such that the small ribosomal subunit fails to associate with the RNA. By including the 5'UTR of RNA4 of alfalfa mosaic virus, we were able to construct an RNA, which when expressed in *X. laevis* oocytes, can be used to screen new ligands which bind to the α9* receptor (* denotes possibility of other subunits). The reasons for the poor ability of α9 receptors (both rat and human) to be expressed in the mammalian cells still remain to be explored.

Transcriptional and translational mechanisms are likely involved in regulation of human and rat α9 subunit expression in native tissues. In the rat adrenal medulla expression levels of α9, α3, and α7 subunits were determined by quantitative PCR (66) and the level was lowest for the α9 subunit. However, the same study showed that transcription of α9, but not α3 and α7 subunits, is upregulated in response to stress. Regulation of transcription and translation of nAChRs may also be relevant in the context of smoking. The concentration of nicotine in active smoker plasma can be 100 nM to 1 μM. Chronic exposure to nicotine leads to activation and desensitization of nAChR subtypes including α4β2 and α7. As a result, the level of expression of α4β2 nAChRs is increased in the brain (147). Smoking is also associated with carcinogenesis, and nicotine-derived metabolites NNK and NNN are considered carcinogenic in lung, breast,

and bladder cancers. α9 receptors mediate cell proliferation of breast cancer cells, and increased α9 nAChR subunit mRNA levels were observed in breast tumor tissues (148). Moreover, α9-nAChR mRNA expression was higher in advanced-stage tumors. It was also shown that nicotine upregulates the mRNA as well as protein level for α9 receptors in breast tumor tissue (148). The mechanism by which nicotine treatment leads to this upregulation remains elusive. α9 subunit expression seems to be important for cell proliferation, and therefore, the mechanisms, whether transcriptional or translational, that control subunit expression might open exciting new avenues for control of tumorigenesis. Our findings suggest the involvement of 5'-untranslated region in the efficient expression of human α9-containing receptors in oocytes. It remains to be investigated whether 5'untransated region contributes to the regulation of translation of α9 subunit *in vivo.*

Table 2.1

Comparison of the functional expression of receptors following co-injection of cRNA for subunits of different species.[a]

Oocyte Batch #	Receptor	Mean current amplitude (nA)	SEM	n
1	hα9rα10	5	1	4
1	rα9hα10	732	155	5
2	hα9rα10	21	7	7
2	rα9hα10	8200	774	6
3	hα9rα10	50	15	6
3	rα9hα10	9755	596	6

[a]Graphical representations of these results are provided in Fig. 2.2.

Table 2.2

Comparison of the functional expression of receptors upon co-injection of different ratios of cRNA for specific subunit.[a]

Receptor	Mean current amplitude (nA)	SEM	n
hα9(1):hα10(1)	142	23	23
hα9(5):hα10(1)	5171	748	21
hα9(1):hα10(5)	6.5	3.9	19

[a]Graphical representations of these results are provided in Fig. 2.3.

Table 2.3

Insertion of AMV improves the expression of human α9 homomeric receptors.[a]

Oocyte Batch #	Receptor	Mean current amplitude (nA)	SEM	n
1	α9	7	4	3
1	α9AMV	268	83	5
2	α9	5	1	5
2	α9AMV	372	52	6
3	α9	8	2	5
3	α9AMV	785	167	10

[a]Graphical representations of these results are provided in Fig. 2.5.

Table 2.4

AMV improves the expression of human α9α10 heteromeric receptors.[a]

Oocyte Batch #	Receptor	Mean current amplitude (nA)	SEM	n
1	hα9α10	43	6	5
1	hα9AMVα10AMV	10813	1739	10
2	hα9α10	60	11	5
2	hα9AMVα10AMV	6999	1627	5
3	hα9α10	237	41	8
3	hα9AMVα10AMV	9763	1379	8

[a]Graphical representations of these results are provided in Fig. 2.5.

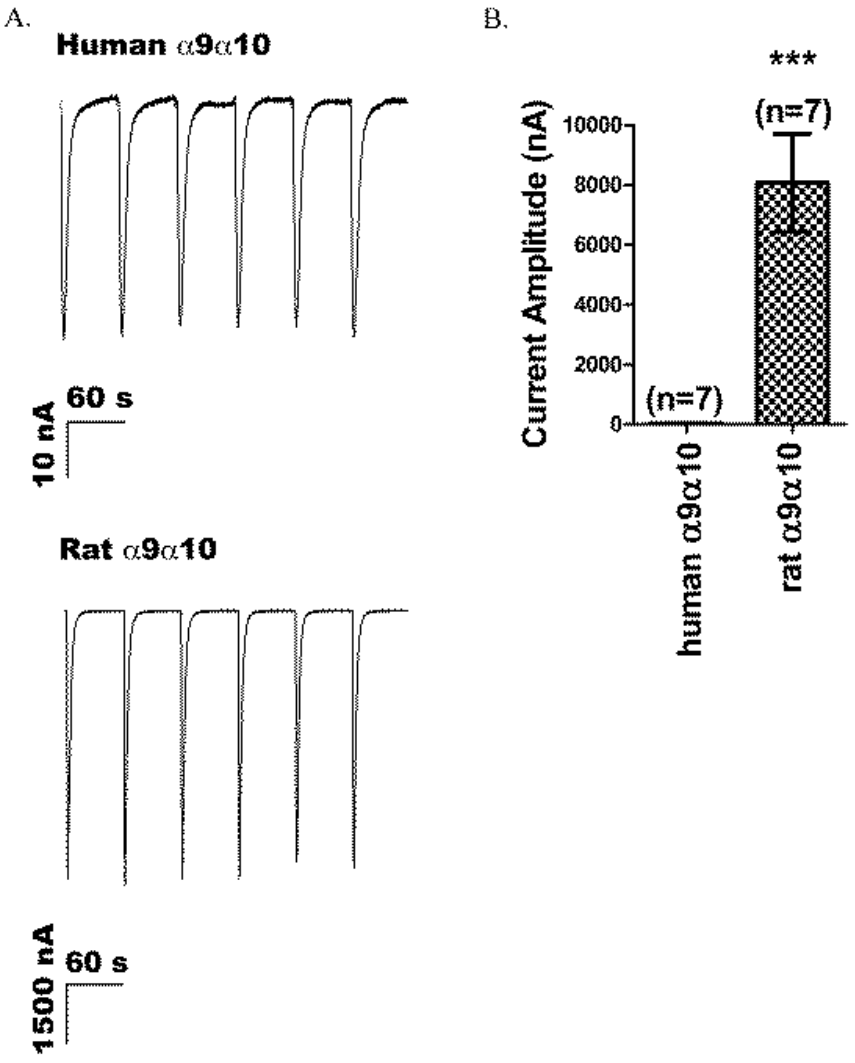

Figure 2.1. Comparison between the levels of exogenous expression of rat and human α9-containing nAChRs in *X. laevis* oocytes.

ACh-gated currents were measured in voltage-clamped oocytes as described in Methods. (A) Representative traces from an oocyte injected with human α9 and human α10 cRNA (top) and rat α9 and rat α10 cRNA (bottom). Robust currents were observed with rat cRNA, but only small currents were observed with human cRNA. (B) Comparison of the averaged current responses evoked by 100 μM ACh applications from oocytes expressing human α9α10 and rat α9α10 receptors. The mean current amplitude was 30 ± 3 nA (n = 7 oocytes) for human α9α10 and 8067 ± 1638 nA (n = 7) for rat α9α10, $p<0.005$. Error bars indicate SEM.

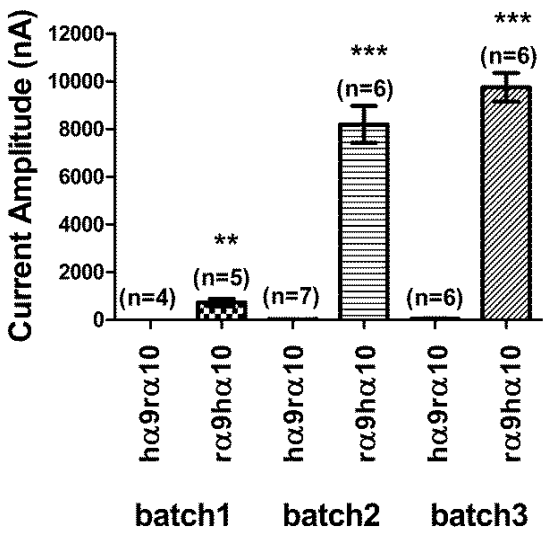

Figure 2.2. Comparison between the level of expression of human α9/rat α10 (hα9rα10) and rat α9/human α10 (rα9hα10) receptors.

Receptors assembled from injection of cRNAs encoding subunits from different species have different levels of functional expression. hα9rα10 nAChRs were expressed with low efficiency compared to rα9hα10. Results from three batches of oocytes are shown. All oocytes of a given batch were injected on the same day and recordings performed 2 days later. Values of mean current amplitudes are given in Table 2.1. **p<0.01. Error bars indicate SEM.

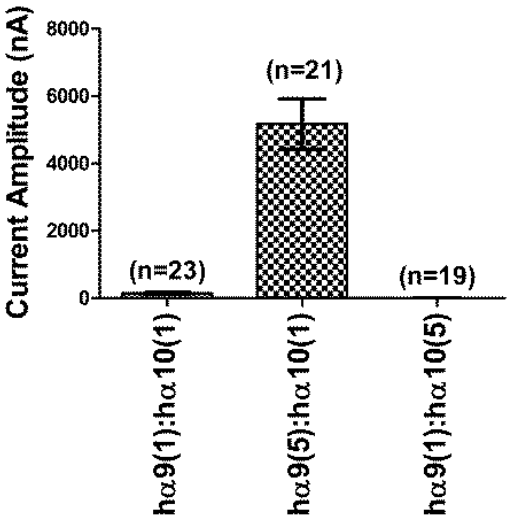

Figure 2.3. Comparison of functional receptor expression following injection of different ratios of receptor subunit cRNA.

Differing subunit ratios of cRNA were injected into oocytes and the resulting levels of expression of functional receptors were compared. Recordings were performed 2 days after injection. The data from oocytes of four different batches were combined to determine the mean current amplitudes. Values are given in Table 2.2. A one-way ANOVA test with Tukey's post-hoc comparison indicated a significant difference between hα9(1):hα10(1) vs. hα9(5):hα10(1), $p<0.001$, and between hα9(5):hα10(1) vs. hα9(1):hα10(5), $p<0.001$. There was no significant difference between hα9(1):hα10(1) and hα9(1):hα10(5), $p>0.05$.

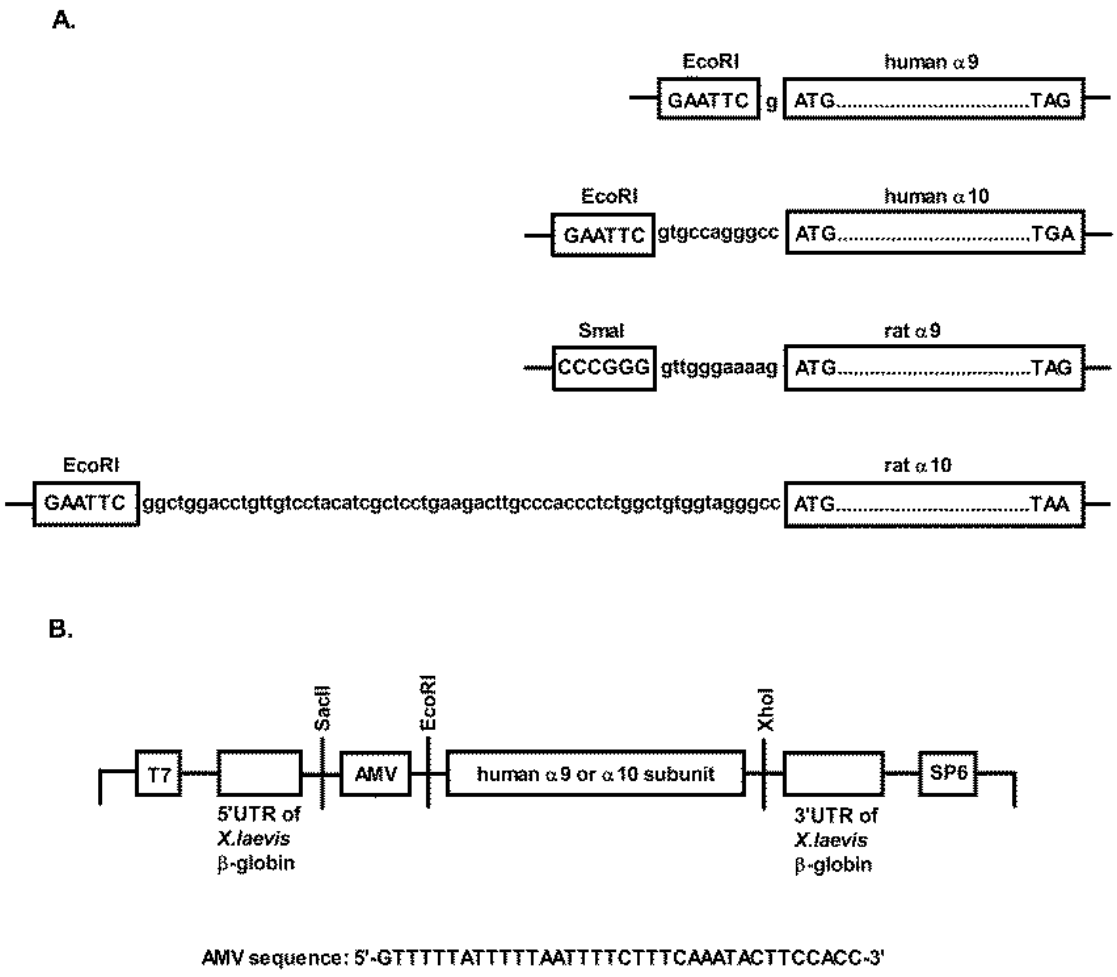

Figure 2.4. Comparison of the 5' untranslated regions in human α9, human α10, rat α9, and rat α10 subunits.

(A) Native 5'UTRs of subunits are between the restriction site and the start codon. (B) The modifications made to the 5' untranslated region of human α9 and α10 subunits are shown. The 5'UTR of RNA4 of the alfalfa mosaic virus coat protein was inserted into the multiple cloning site of the pSGEM vector between SacII and EcoRI sites. The subunit-encoding sequence is between the EcoRI and XhoI sites.

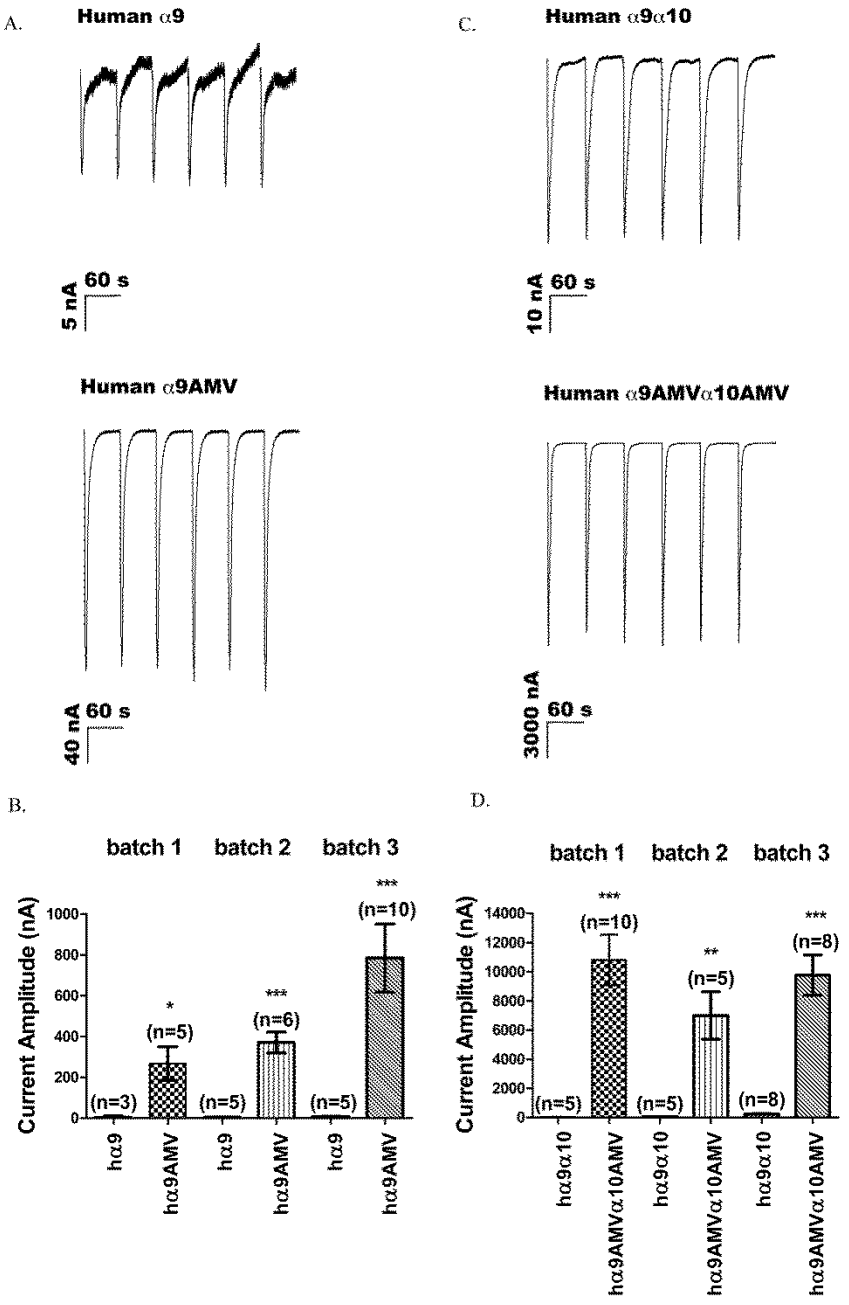

Figure 2.5. AMV improves the level of functional expression of α9-containing nAChRs.

(A) Representative traces and (B) comparisons of the levels of functional expression of homomeric human α9 receptors encoded by cRNA without (A, top) and with (A, bottom) AMV. The results are from three different batches of oocytes, each isolated from a different frog and recorded on 3rd day after injection, are presented. (C and D) Comparison of the level of expression of heteromeric receptors. Recordings were conducted on the second day after injection. Values for mean current amplitude are shown in Tables 2.3 and 2.4. *p<0.05; **p<0.01. Error bars indicate SEM.

CHAPTER 3

INTERACTION BETWEEN NICOTINIC ACETYLCHOLINE RECEPTORS AND PURINERGIC RECEPTORS

Introduction

Neuronal nAChRs are present ubiquitously throughout the CNS. Presynaptically located receptors modulate release of neurotransmitters such as glutamate, serotonine and dopamine (149-152). Activation of postsynaptically located nAChRs causes depolarization, increase in intracellular calcium and activation of intracellular signaling mechanisms (3). The organization of the nervous system is so complex that a single nerve terminal might harbor different classes of receptors, such as purinergic and nAChRs (153).

Purinergic P_2X receptors are ionotropic channels permeable to cations. They have trimeric organization with homomeric (P_2X_1-P_2X_5, P_2X_7) or heteromeric ($P_2X_{1/2}$, $P_2X_{1/4}$, $P_2X_{1/5}$, $P_2X_{2/3}$, $P_2X_{2/6}$, $P_2X_{4/6}$) structure formed from P_2X_1- P_2X_7 subunits (154-156). These receptors are expressed throughout body and are involved in pain, inflammation, cancer and other pathophysiological processes (157-161).

nAChRs and purinergic receptors colocalize in several brain regions as well as outside of the CNS. For example, nAChRs colocalize with P_2X receptors in the guinea pig myenteric neurons, in rat and guinea pig sympathetic neurons, and the receptors physically interact with each other (162-165). The nicotinic and purinergic receptors interact to control the release of glutamate in hippocampus (166).

In outer hair cells the α9α10 nAChR mediates synaptic transmission between efferent olivocochlear neurons and outer hair cells (167). There are several purinergic receptors present in outer hair cells along with α9α10 nAChRs. Among them are ionotropic P_2X_1, P_2X_2, P_2X_4, and to a lesser degree P_2X_7, and metabotropic P_2Y_1, P_2Y_2, and P_2Y_4 receptors (168). It was shown that ATP- induced Ca^{2+} rise in outer hair cells is

inhibited by acetylcholine, and this effect is sensitive to α-bungarotoxin (169) suggesting an interplay between nicotinic and purinergic receptors. One possible pair that could interact with each other includes α9α10 nicotinic receptor and P_2X_4 purinergic receptor.

Immune cells are another location where nicotinic and purinergic receptors colocalize. mRNAs of different nAChRs were detected in immune cells. Transcripts for nicotinic α2, α5, α6, α7, α10, and β2 subunits were found by RT-PCR in mononuclear leukocytes, bone-marrow derived dendritic cells and macrophages of C57BL/6J mice (170). Expression of α9 and α10 subunits was demonstrated in human T- and B-lymphocytes (171). The activation of the α7 receptor is believed to have anti-inflammatory effects (172,173). The role of α9α10 nAChRs in immune cells is at the beginning of being understood. It was shown in several studies that α9α10 antagonists reduce the number of immune cells at the site of injury in an animal model of neuropathic pain (70). Also, a recent study showed that onset of experimental autoimmune encephalomyelitis is delayed and the severity of the disease is attenuated in α9 knockout mice, an observation suggesting involvement of the α9 subunit in proinflammatory mechanisms (174).

Among purinergic P_2X receptors, the predominant subtype present in immune cells includes P_2X_7 (175,176). Activation of this receptor leads to increased release of the proinflammatory cytokine interleukin-1β (177). The genetic ablation of P_2X_7 receptors results in reduced chronic inflammatory and neuropathic pain (178-180) as well as in suppressed development of experimental autoimmune encephalomyelitis (181), but see Chen et al. (182). Together with P_2X_7, P_2X_4 is also believed to play an important role in immune processes (183). P_2X_4 receptors of peritoneal macrophages mediate

prostaglandin E2 (PGE2) release via phosphorylation of p38MAPK which leads to inflammatory pain initiation (184). The inhibition of the P_2X_4 receptor has anti-inflammatory effects. For example, genetic ablation of the P_2X_4 receptor prevents pain hypersensitivity in inflammation (185).

We investigated the idea that α9α10 nAChRs interact with P_2X_4 receptors and/or with P_2X_7 receptors. The interaction was tested by evaluating the character of response from coapplication of ACh and ATP when two receptors are coexpressed in oocytes of *Xenopus laevis.* We thought if the receptors interact and one inhibits another then the current response from coapplication of both agonists will be a fraction of the predicted summation of responses from individual agonists. We also compared the agonist sensitivities for both receptors when they were present alone in oocytes or when α9α10 and P_2X_4, as well as α9α10 and P_2X_7 receptors were coexpressed.

Materials and methods

cRNA preparation and injection

cDNA for rat α9 and α10 subunits were provided by A.B.Elgoyhen (Universidad de Buenos Aires, Buenos Aires, Argentina), and were in pGEMHE and pSGEM vectors, respectively. cDNAs encoding rat P_2X_4 and P_2X_7 were provided by Daryl Davies (University of Southern California, Los Angeles, CA) in pcDNA3 vector (Invitrogen, Carlsbad, CA). cRNAs were *in vitro* transcribed using T7 mMessage mMachine kit (Ambion, Austin, TX) from linearized cDNAs. The concentration of cRNA was determined spectrophotometrically at 260 nm.

Two-electrode voltage clamp

Oocytes of stage IV-V were dissected from African clawed frog following the protocol described in details elsewhere (15). Oocytes were injected with 10 – 60 ng/oocyte of cRNA. The injected oocytes were kept in ND96 solution (96 mM NaCl, 1.8 mM $CaCl_2$, 2 mM KCl, 1.0 mM $MgCl_2$, 5 mM HEPES, pH 7.1-7.5) supplemented with antibiotics (50 U/mL penicillin, 50 μg/mL streptomycin, 50 μg/mL gentamicin). The recordings were conducted 1-6 days after injection.

Two-electrode voltage clamp was done as described in the literature (15) using voltage-clamp amplifier (OC-725B, Warner Instrument Corporation, Hamden, CT). The membrane potential was kept at -70 mV. The oocytes were placed into ~200 μL bath custom made out of pipette tip and perfused with ND96 or barium-substituted ND96 (96 mM NaCl, 1.8 mM $BaCl_2$, 2 mM KCl, 1.0 mM $MgCl_2$, 5 mM HEPES, pH 7.1-7.5). Agonists were bath applied automatically by pump in the volume of 20 μL while the solution flow was stopped.

For concentration-response curve determination, agonists of increasing concentrations were delivered manually in a volume of 20 μL while the flow of solution was stopped. The agonists concentration-response curves were fit using sigmoidal curve-fitting function of PRISM program to determine half-maximal effective concentration (EC_{50}) values.

Results

Interaction between rat α9α10 and rat P_2X_4 receptors

α9α10 nAChRs co-localize with P_2X_4 receptors in several places, such as outer hair cells and immune cells. In outer hair cells ACh inhibits ATP-evoked response (169).

We tested the hypothesis of interaction between rat α9α10 and purinergic P_2X_4 receptors. Acetylcholine activates rat α9α10 receptors with an EC_{50} value of 13.8 μM (78). In our experiments we used 100 μM agonists in order to activate receptors. P_2X_4 receptors are activated by ATP with EC_{50} value equal to 6.9 ± 0.8 μM (186). 100 μM ATP was used to activate P_2X_4 receptors. Agonists were delivered individually in a bolus of 20 μL to activate either α9α10 or P_2X_4 receptors. This was followed by 20 μL application of both agonists at 100 μM concentration each. We assumed that if receptors function independently, then the resultant current from coapplication of agonists ($I_{ACh/ATP}$) would be approximately equal to the sum of currents from each agonist (I_{ACh} + I_{ATP}), the so called predicted current. If one receptor inhibits another, then the actual current from coapplication of agonists would be less than the predicted current.

When tested under similar conditions, oocytes showed inconsistent results. Roughly half of the tested oocytes (n=6) had currents from agonist coapplication less than the predicted currents, suggesting inhibition (Fig. 3.1 and Table 3.1). The actual current was 76% of predicted current. Another half of oocytes (n=6) showed a purely additive character of current, suggesting independent function for receptors (Fig. 3.2 and Table 3.2). The actual currents in these oocytes were equal to or even exceeded the predicted currents.

Due to the inconsistency in the results we undertook an alternative approach. We measured agonist sensitivities for both α9α10 and P_2X_4 receptors under two experimental conditions: when receptors were present alone in oocytes and when they were coexpressed. We assumed that if receptors were physically coupled to each other, then agonist sensitivity of one might be affected by the presence of another receptor even when the other receptor is not activated. The results indicated ~1.6-fold rightward shift in ATP sensitivity for P_2X_4 receptors when they were coexpressed with α9α10 receptors (Fig. 3.3 and Table 3.3) with EC_{50} equal to 10 μM for P_2X_4 receptors alone and 16 μM for P_2X_4 receptors coexpressed with nicotinic receptors (all measurement were conducted in regular ND96 solution). The ACh sensitivities measured on rat α9α10 receptors were similar when receptors were expressed alone (EC_{50} = 15 μM) and when they were coexpressed (EC_{50} = 11 μM) (Fig. 3.3 and Table 3.4).

Oocytes of *Xenopus laevis* frog are used routinely as a heterologous system to study different receptors and channels. The advantage of oocytes is in relative absence of endogenous channels that might influence the results of the studies. However, oocytes do express endogenous calcium-sensitive chloride-channels ($I_{Cl(Ca)}$) (187-189) that might interfere with the recordings from calcium-permeable receptors such as α9α10 and P_2X_4 (190). In order to avoid contribution of $I_{Cl(Ca)}$ to the results we repeated the above experiment in Ba-substituted ND96, where 1.8 mM $CaCl_2$ was replaced by 1.8 mM $BaCl_2$.

The results were similar to the results in normal ND96 for P_2X_4 and α9α10 receptors (Fig 3.3 and Tables 3.3 and 3.4). The EC_{50} for ATP on P_2X_4 receptors alone was 9.8 μM and for P_2X_4 receptors coinjected with α9α10 receptors - 16 μM. We

observed reduction in ACh sensitivity on α9α10 receptors in the presence of barium, in regular ND96 the EC_{50} was equal to 15 μM compared to 49 μM in Ba-ND96. For α9α10 receptors coexpressed together with P_2X_4 receptors, the ACh EC_{50} increased from 11 μM to 55 μM when calcium was substituted with barium (Fig. 3.4 and Table 3.4). EC_{50}s for ATP on P_2X_4 receptors were similar in regular and Ba-ND96 (Fig. 3.3 and Table 3.3).

Interaction between rat α9α10 and P_2X_7 receptors

P_2X_7 receptors are the predominant purinergic receptor subtype present in immune cells, such as lymphocytes, macrophages/monocytes, and mast cells where they mediate release of proinflammatory cytokines (155,177,191). Immune cells also express subunits for nicotinic acetylcholine receptor (170,192,193). Recent work by Mikulski et al. (194) suggested possible interplay between nicotinic and purinergic receptors in rat alveolar macrophages. Even though the authors were not able to record ACh-evoked current from macrophages, and involvement of metabotropic P_2Y receptors was suggested, we tested the hypothesis of interaction between α9α10 and P_2X_7 receptors.

P_2X_7 receptors are unique among all other purinergic P_2X receptors in their ability to change permeability to different ions with prolonged activation time (155). These receptors are highly permeable to calcium ions and less sensitive to agonist ATP compared to other P_2X receptors with EC_{50} ranging from 2 to 4 mM depending on the report (195). In our study we used 1 mM ATP to activate receptors. Due to high calcium permeability of both P_2X_7 and α9α10 receptors and possibility of interference from calcium-sensitive chloride channels endogenously expressed by oocytes, we conducted experiments in barium-substituted ND96.

The average current amplitude for rat P_2X_7 receptors when activated by 1 mM ATP was relatively low compared to rat α9α10 nAChRs activated by 100 μM ACh in barium-containing ND96, which makes comparison between predicted current and actual current from coapplication of both agonists difficult. We therefore also used 10 mM choline to activate rat α9α10 receptors. Choline is a partial agonist of rat α9α10 receptors, with an EC_{50} equal to 3 μM (78). The results demonstrated lack of interaction between two receptors, with current from coapplication of agonists equal to the sum of responses from individual agonists (Figure 3.5 and Table 3.5).

We also measured agonist sensitivities for ACh and ATP on rat α9α10 and P_2X_7 receptors under two experimental conditions: when receptors were expressed alone in oocytes and when they were coexpressed. The EC_{50} were similar for both agonists independent of whether the receptors were alone or coinjected. The ACh EC_{50} on rat α9α10 alone was equal to 40 μM, n=8, and it was 46 μM, n=7 when receptors were coexpressed together with P_2X_7. The ATP EC_{50} was 2.2 mM, n=3 for P_2X_7 alone and 1.6 mM, n=6 for P_2X_7 coinjected with rat α9α10 receptor (Figure 3.6 and Tables 3.6 and 3.7).

Discussion

The main conclusion from the study is that we were unable to find conclusive and highly reproducible evidence that would demonstrate interaction between rat α9α10 and P_2X_4 receptors or between rat α9α10 and P_2X_7 receptors. The variability in the results with coapplication of agonists in case of α9α10 - P_2X_4 pair might point to the inability of the currently used heterologous expression system to detect interaction in all instances. The variation in the results could be explained by the different level of plasma membrane channel density if physical interaction between receptors takes place. If this is the case,

then the interaction can be detected only when the level of receptor expression is high enough to guarantee juxtaposition of interacting receptors. The dependence of detection of cross-inhibition on the channel membrane density was suggested for α3β4 – P_2X_2 interaction (163).

The slight (1.6-fold) rightward shift in the ATP sensitivity for rat P_2X_4 receptors when they were coexpressed with rat α9α10 receptors compared to when they were alone might be within experimental error as far as the ATP EC_{50} in the literature ranges from 1 to 10 μM (196-199). However, the persistent character of the shift, observed in regular ND96 as well as in barium-substituted ND96 could point to the influence from α9α10 nAChRs. The changes in agonist sensitivities for both ACh and ATP were observed for rat α3β4 and P_2X_2 receptors expressed heterologously in HEK293 cells (164). These changes were explained by ability of one receptor to inhibit another even without being activated.

Nicotinic acetylcholine and purinergic receptors belong to two distinct classes of ligand-activated ion-channels. Despite their structural and pharmacological differences, they are involved in similar physiological processes. For example, activation of P_2X_7 purinergic receptors in immune cells leads to increase in release of proinflammatory IL-1β cytokine. Similar to purinergic receptors, α9 subunit might also be involved in proinflammatory mechanisms (174). The presence of unrelated receptors in similar locations and action of ACh and ATP as cotransmitters raise questions about the possibility of functional interaction between receptors. For example, nicotinic and purinergic receptors are present on presynaptic membranes of glutamatergic neurons of hippocampus where they modulate neurotransmitter release (166). Located on

sympathetic neurons, nicotinic and purinergic receptors inhibit each other, as was shown for rat and guinea pig neurons (200,201).

Nicotinic and purinergic receptors are colocalized and physically interact with each other in myenteric neurons. In cultured myenteric neuons as well as in HEK-293 cells expressing α3β4 and P_2X_2 receptors coapplication of 3 mM ACh and 1 mM ATP evokes current which is a fraction of predicted summary response assuming that receptors function independently (162). The mechanism by which two receptors interact is through physical interaction where the intracellular loop of the nAChR interacts with the C-terminus of the purinergic receptor (164). Inhibitory interactions between rat α3β4 and P_2X_2 as well as between α3β4 and P_2X_4 receptors were also shown in *Xenopus laevis* oocytes (163). Fluorescence resonance energy transfer analysis showed that α4β2 and P_2X_2 receptors are localized within 100 nm from each other (202).

The colocalization of receptors belonging to different families, such as purinergic and nicotinic acetylcholine is intriguing as far as neurotransmitters activating both receptors can be present simultaneously. For example, during inflammation, ATP as well as ACh is present at the site of injury. When both agonists are present, they can activate highly calcium-permeable receptors (α7 and α9α10 as well as P_2X_4 and P_2X_7) leading to the amplified increase in calcium influx. The inhibitory interaction between nicotinic and purinergic receptors could be a mechanism by which calcium-ion flow and neuronal depolarization are regulated.

Table 3.1

Results suggesting inhibition.

Oocyte #	I_{ACh}, -nA	SEM	I_{ATP}, -nA	SEM	$I_{ACh/ATP}$ predicted, -nA	$I_{ACh/ATP}$ actual, -nA	SEM	% of predicted
1	9041	213	3071	114	12179	9517	72	78
2	16321	580	8408	423	24729	16931	545	68
3	23811	315	7451	458	31263	25093	512	80
4	15620	905	9809	409	25429	20752	613	82
5	12251	212	14173	102	26424	17634	187	67
6	10270	32	4276	101	14546	12322	231	85

Table 3.2

Results suggesting independent function

Oocyte #	I_{ACh}, -nA	SEM	$I_{ATP,}$ -nA	SEM	$I_{ACh/ATP}$ predicted, -nA	$I_{ACh/ATP}$ actual, -nA	SEM	% of predicted
1	4185	394	3077	104	7262	9270	267	128
2	634	23	470	17	1104	2877	100	261
3	3656	220	2771	103	6427	11468	297	178
4	225	5	525	31	750	1065	47	142
5	8828	205	4031	204	12859	13678	212	106
6	6217	86	787	8	7004	6853	291	98

Table 3.3

EC_{50} values for ATP on rat P_2X_4 receptors under different experimental conditions.

Solution	Receptor	EC50, μM	95% CI, μM	Hillslope	95% CI	n
ND96	P2X4	10	6-17	1.5	0.5-2.5	3
ND96	α9α10 + P2X4	16	12-20	1	0.8-1.4	6
Ba-ND96	P2X4	9.8	9-10	1.7	1.5-1.8	16
Ba-ND96	α9α10 + P2X4	16	14-17	1.2	1.1-1.3	14

Table 3.4

EC_{50} values for ACh on rat α9α10 receptors under different experimental conditions.

Solution	Receptor	EC50, μM	95% CI, μM	Hillslope	95% CI	n
ND96	α9α10	15	13-17	1.5	1.2-1.7	3
ND96	α9α10 + P2X4	11	9-13	1.4	1-1.7	7
Ba-ND96	α9α10	49	41-59	0.8	0.7-0.9	6
Ba-ND96	α9α10 + P2X4	55	45-67	0.9	0.7-1	4

Table 3.5

Analysis of possible interaction between rat α9α10 and rat P_2X_7 receptors in barium-containing ND96.

Oocyte #	$I_{Choline}$, -nA	SEM	I_{ATP}, -nA	SEM	$I_{Choline/ATP}$ predicted -nA	$I_{Choline/ATP}$ actual -nA	SEM	% of predicted
1	301	6	275	13	576	545	4	95
2	353	6	307	6	660	622	9	94
3	462	9	707	27	1169	1096	57	94

Table 3.6

EC_{50} for ACh on rat α9α10 alone and coinjected with rat P_2X_7 in Ba-ND96.

Receptor	EC50, μM	95% CI	Hillslope	95% CI	n
α9α10	40	38-42	1.1	1.0-1.2	8
α9α10 + P2X7	46	43-48	1.1	1.0-1.2	7

Table 3.7

EC_{50} for ATP on rat P_2X_7 alone and coinjected with rat α9α10 in Ba-ND96.

Receptor	EC50, mM	95% CI	Hillslope	95% CI	n
P2X7	2.2	2.1-2.3	1.4	1.3-1.5	3
P2X7 + α9α10	1.6	1.4-1.8	1.4	1.1-1.6	6

A.

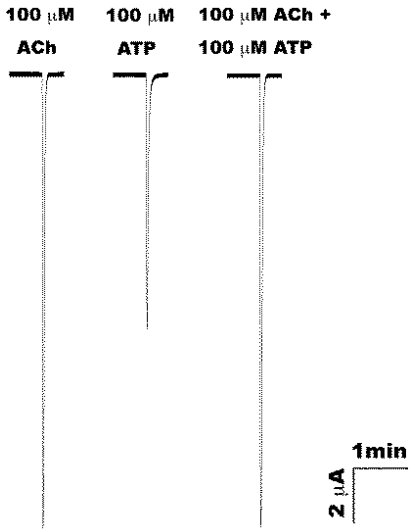

B.

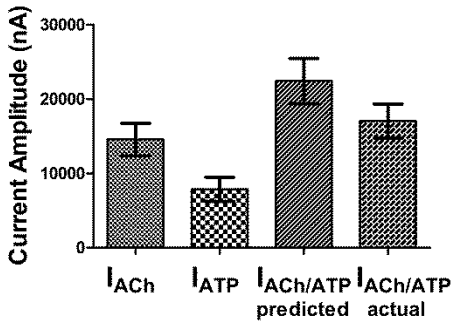

Figure 3.1 Representative traces (A) and bar graph (B) summarizing the results suggesting interaction between rat α9α10 and P_2X_4 receptors. A) The actual $I_{ACh/ATP}$ is smaller than the predicted current (I_{ACh} + I_{ATP}) suggesting inhibition between receptors. B) The data are a summary from six oocytes' individual values which are presented in Table 3.1. I_{ACh} = 14552 ± 2191 nA; I_{ATP} = 7865 ± 1632 nA; $I_{ACh/ATP}$ predicted = 22417 ± 3038 nA ; $I_{ACh/ATP}$ actual = 17042 ± 2294 nA. The oocytes were injected with 10 – 60 ng/oocyte of RNA, and with 1:1 ratio for α9 and α10 subunits. The recordings were conducted 1 to 6 days post/injection. The delivery of agonists was according to the procedure described in *Materials and methods*. There is a ns difference between $I_{ACh/ATP}$ predicted and $I_{ACh/ATP}$ actual, $p>0.05$ assessed by *t-test*.

A.

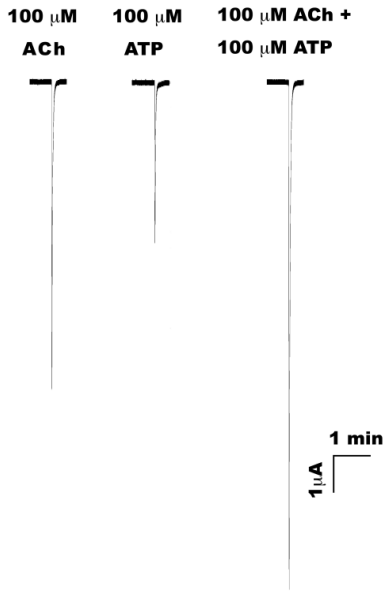

B.

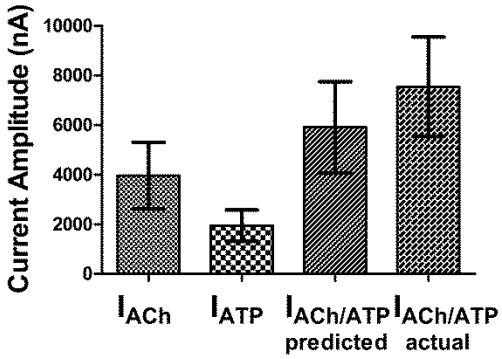

Figure 3.2 Representative traces (A) and bar graph (B) summarizing the results suggesting independent function of rat α9α10 and P_2X_4 receptors heterologously expressed in oocytes of *Xenopus laevis* frog. A) The actual $I_{ACh/ATP}$ is bigger (130%) than the predicted current (I_{ACh} + I_{ATP}) suggesting no inhibition between receptors. B) The data are a summary from six oocytes, individual values for which are presented in Table 3.2. I_{ACh} = 3958 ± 1341 nA; I_{ATP} = 1941 ± 628 nA; $I_{ACh/ATP}$ predicted = 5901 ± 1838 nA ; $I_{ACh/ATP}$ actual = 7535 ± 2002 nA. The oocytes were injected with 13 – 53 ng/oocyte of RNA, and with 1:1 ratio for α9 and α10 subunits. The recordings were conducted 1 to 3 days post/injection.

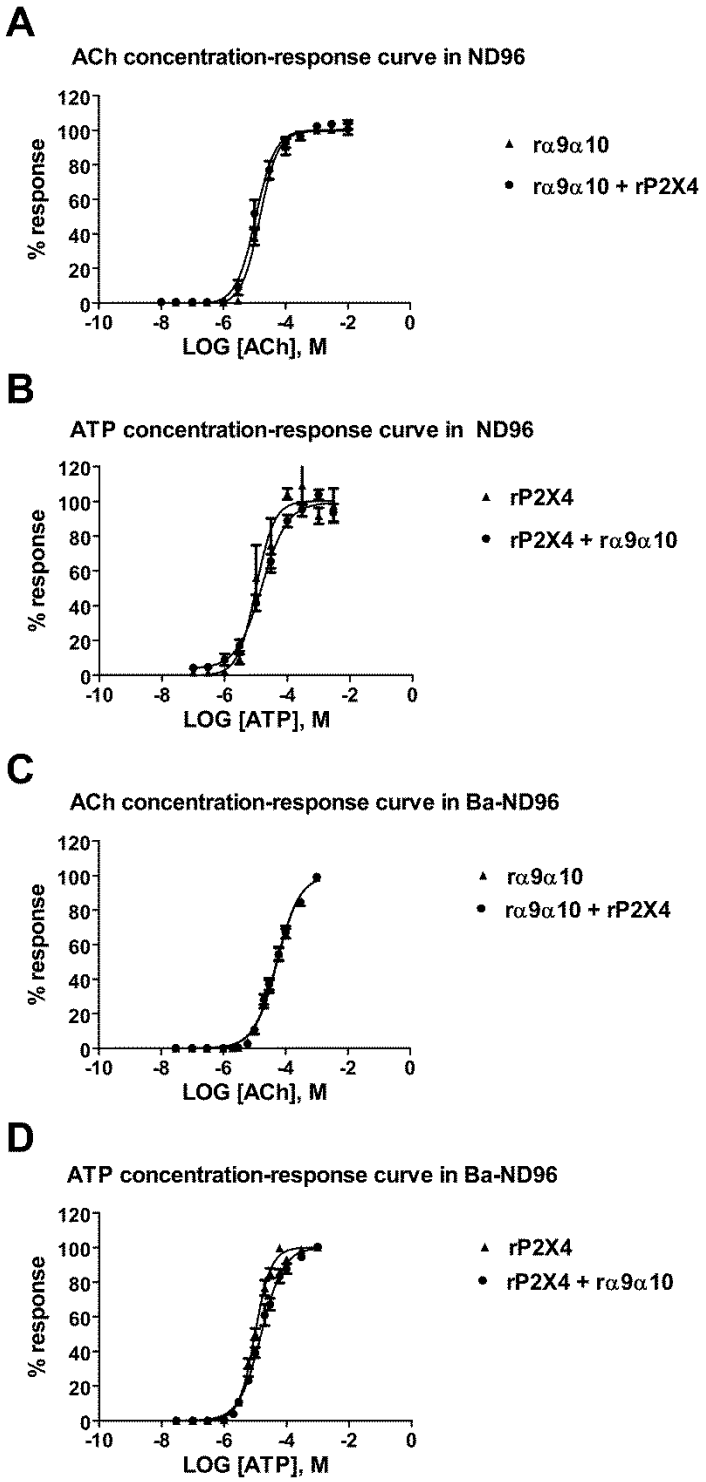

Figure 3.3 Concentration-response curves for ACh and ATP. EC_{50}s for ACh and ATP on rα9α10 and P_2X_4 were determined under two experimental conditions: when receptors were alone and when they were coexpressed. The experiments were conducted in regular ND96 and in barium-substituted ND96. The values are presented in Tables 3.3 and 3.4.

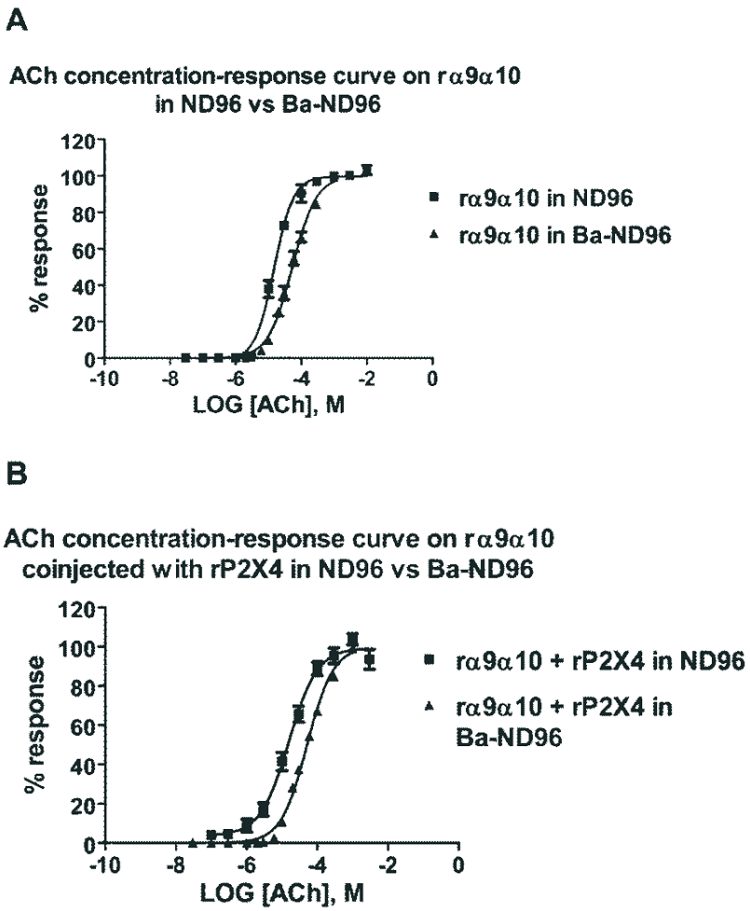

Figure 3.4 Comparison between ACh EC_{50} in calcium vs. barium-containing ND96. When calcium chloride was substituted with barium chloride the EC_{50} shifted to the right. The above curves are the same as curves in Figure 3.3 but taken in pairs for comparison.

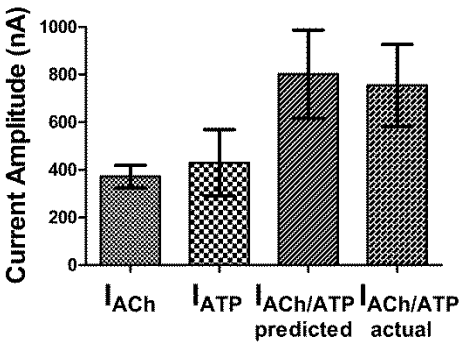

Figure 3.5 Graphical representation of results for rat α9α10 – P_2X_7 interaction. The data are a summary from three oocytes individual values of which are presented in Table 3.5. $I_{ACh/}$ = 372 ± 47 nA. I_{ATP} = 430 ±139 nA. $I_{ACh/ATP}$ predicted = 802 ± 185 nA. $I_{ACh/ATP}$ actual = 754 ± 172 nA. The oocytes were injected with 20 ng/oocyte of α9 RNA, 21 ng/oocyte of α10 RNA, and 41 ng/oocyte of P_2X_7 RNA.The recordings were conducted 2-3 days post/injection. There is nonsignificant difference between $I_{ACh/ATP}$ predicted and $I_{ACh/ATP}$ actual, $p>0.05$, assessed by *t-test.*

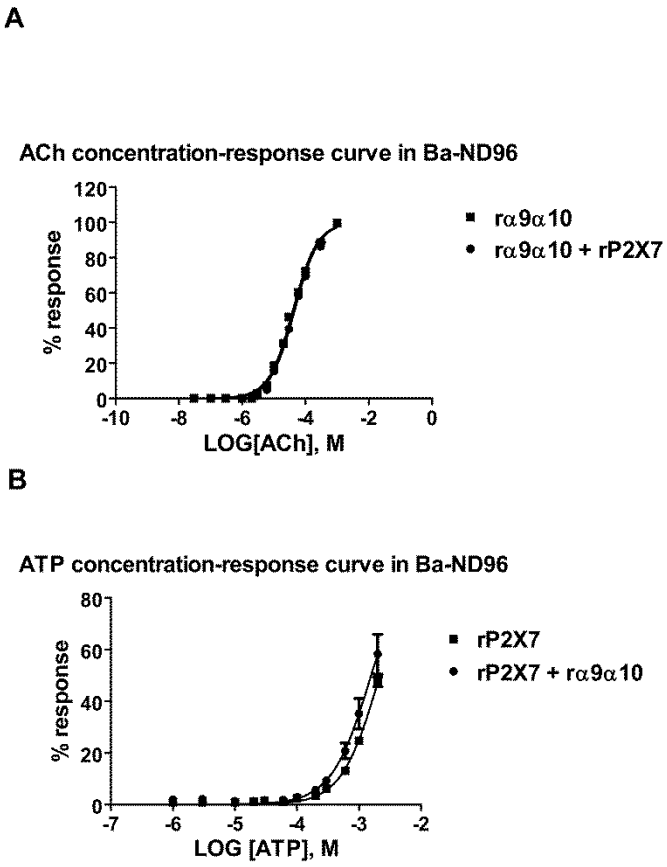

Figure 3.6 Concentration-response curves for ACh and ATP on rat α9α10 and rat P_2X_7. A) Concentration-response curve for ACh EC_{50} on rat α9α10 expressed alone in oocytes is identical to the curve for ACh EC_{50} on rat α9α10 coexpressed with rat P_2X_7 receptors. The EC_{50} values are presented in Table 3.6. B) Similar to ACh, ATP activates rat P_2X_7 receptors with similar potency independent whether receptors are alone or coexpressed with α9α10 receptors. The values for EC_{50}s and Hillslopes with 95% CI are presented in Table 3.7.

REFERENCES

1. Karlin, A. (2002) Emerging structure of the nicotinic acetylcholine receptors. Nat Rev Neurosci **3**, 102-114

2. McGehee, D. S. (1999) Molecular diversity of neuronal nicotinic acetylcholine receptors. Ann N Y Acad Sci **868**, 565-577

3. Dani, J. A., and Bertrand, D. (2007) Nicotinic acetylcholine receptors and nicotinic cholinergic mechanisms of the central nervous system. Annu Rev Pharmacol Toxicol **47**, 699-729

4. Kawashima, K., and Fujii, T. (2008) Basic and clinical aspects of non-neuronal acetylcholine: overview of non-neuronal cholinergic systems and their biological significance. J Pharmacol Sci **106**, 167-173

5. Wessler, I., Kilbinger, H., Bittinger, F., Unger, R., and Kirkpatrick, C. J. (2003) The non-neuronal cholinergic system in humans: expression, function and pathophysiology. Life Sci **72**, 2055-2061

6. Gotti, C., and Clementi, F. (2004) Neuronal nicotinic receptors: from structure to pathology. Prog Neurobiol **74**, 363-396

7. Newhouse, P., Singh, A., and Potter, A. (2004) Nicotine and nicotinic receptor involvement in neuropsychiatric disorders. Curr Top Med Chem **4**, 267-282

8. Unwin, N. (2005) Refined structure of the nicotinic acetylcholine receptor at 4A resolution. J Mol Biol **346**, 967-989

9. Ulens, C., Akdemir, A., Jongejan, A., van Elk, R., Bertrand, S., Perrakis, A., Leurs, R., Smit, A. B., Sixma, T. K., Bertrand, D., and de Esch, I. J. (2009) Use of acetylcholine binding protein in the search for novel alpha7 nicotinic receptor ligands. In silico docking, pharmacological screening, and X-ray analysis. J Med Chem **52**, 2372-2383

10. Terlau, H., and Olivera, B. M. (2004) Conus venoms: a rich source of novel ion channel-targeted peptides. Physiol Rev **84**, 41-68

11. Azam, L., and McIntosh, J. M. (2009) Alpha-conotoxins as pharmacological probes of nicotinic acetylcholine receptors. Acta Pharmacol Sin **30**, 771-783

12. Olivera, B. M., Quik, M., Vincler, M., and McIntosh, J. M. (2008) Subtype-selective conopeptides targeted to nicotinic receptors: Concerted discovery and biomedical applications. Channels (Austin) **2:143-52**

13. McIntosh, J. M., Yoshikami, D., Mahe, E., Nielsen, D. B., Rivier, J. E., Gray, W. R., and Olivera, B. M. (1994) A nicotinic acetylcholine receptor ligand of unique specificity, alpha-conotoxin ImI. J Biol Chem **269**, 16733-16739

14. Ellison, M., Gao, F., Wang, H. L., Sine, S. M., McIntosh, J. M., and Olivera, B. M. (2004) Alpha-conotoxins ImI and ImII target distinct regions of the human alpha7 nicotinic acetylcholine receptor and distinguish human nicotinic receptor subtypes. Biochemistry **43**, 16019-16026

15. Cartier, G. E., Yoshikami, D., Gray, W. R., Luo, S., Olivera, B. M., and McIntosh, J. M. (1996) A new alpha-conotoxin which targets alpha3beta2 nicotinic acetylcholine receptors. J Biol Chem **271**, 7522-7528

16. McIntosh, J. M., Azam, L., Staheli, S., Dowell, C., Lindstrom, J. M., Kuryatov, A., Garrett, J. E., Marks, M. J., and Whiteaker, P. (2004) Analogs of alpha-conotoxin MII are selective for alpha6-containing nicotinic acetylcholine receptors. Mol Pharmacol **65**, 944-952

17. Ellison, M., Haberlandt, C., Gomez-Casati, M. E., Watkins, M., Elgoyhen, A. B., McIntosh, J. M., and Olivera, B. M. (2006) Alpha-RgIA: a novel conotoxin that specifically and potently blocks the alpha9alpha10 nAChR. Biochemistry **45**, 1511-1517

18. Azam, L., Dowell, C., Watkins, M., Stitzel, J. A., Olivera, B. M., and McIntosh, J. M. (2005) Alpha-conotoxin BuIA, a novel peptide from Conus bullatus, distinguishes among neuronal nicotinic acetylcholine receptors. J Biol Chem **280**, 80-87

19. Walker, C. S., Steel, D., Jacobsen, R. B., Lirazan, M. B., Cruz, L. J., Hooper, D., Shetty, R., DelaCruz, R. C., Nielsen, J. S., Zhou, L. M., Bandyopadhyay, P., Craig, A. G., and Olivera, B. M. (1999) The T-superfamily of conotoxins. J Biol Chem **274**, 30664-30671

20. Chi, S. W., Kim, D. H., Olivera, B. M., McIntosh, J. M., and Han, K. H. (2006) NMR structure determination of alpha-conotoxin BuIA, a novel neuronal nicotinic acetylcholine receptor antagonist with an unusual 4/4 disulfide scaffold. Biochem Biophys Res Commun **349**, 1228-1234

21. Stone, B. L., and Gray, W. R. (1982) Occurence of hydroxyproline in a toxin from the marine snail Conus geographus. Arch. Biochem. Biophys. **216**, 756-767

22. Carter, P. J., Winter, G., Wilkinson, A. J., and Fersht, A. R. (1984) The use of double mutants to detect structural changes in the active site of the tyrosyl-tRNA synthetase (Bacillus stearothermophilus). Cell **38**, 835-840

23. Shiembob, D. L., Roberts, R. L., Luetje, C. W., and McIntosh, J. M. (2006) Determinants of alpha-conotoxin BuIA selectivity on the nicotinic acetylcholine receptor beta subunit. Biochemistry **45**, 11200-11207

24. Hidalgo, P., and MacKinnon, R. (1995) Revealing the architecture of a K^+ channel pore through mutant cycles with a peptide inhibitor. Science **268**, 307-310

25. Loughnan, M. L., Nicke, A., Jones, A., Adams, D. J., Alewood, P. F., and Lewis, R. J. (2004) Chemical and functional identification and characterization of novel sulfated alpha-conotoxins from the cone snail Conus anemone. J Med Chem **47**, 1234-1241

26. Luo, S., Kulak, J. M., Cartier, G. E., Jacobsen, R. B., Yoshikami, D., Olivera, B. M., and McIntosh, J. M. (1998) alpha-conotoxin AuIB selectively blocks alpha3 beta4 nicotinic acetylcholine receptors and nicotine-evoked norepinephrine release. J Neurosci **18**, 8571-8579

27. Martinez, J. S., Olivera, B. M., Gray, W. R., Craig, A. G., Groebe, D. R., Abramson, S. N., and McIntosh, J. M. (1995) alpha-Conotoxin EI, a new nicotinic acetylcholine receptor antagonist with novel selectivity. Biochemistry **34**, 14519-14526

28. Loughnan, M., Bond, T., Atkins, A., Cuevas, J., Adams, D. J., Broxton, N. M., Livett, B. G., Down, J. G., Jones, A., Alewood, P. F., and Lewis, R. J. (1998) alpha-conotoxin EpI, a novel sulfated peptide from Conus episcopatus that selectively targets neuronal nicotinic acetylcholine receptors. J Biol Chem **273**, 15667-15674

29. McIntosh, J. M., Dowell, C., Watkins, M., Garrett, J. E., Yoshikami, D., and Olivera, B. M. (2002) Alpha-conotoxin GIC from Conus geographus, a novel peptide antagonist of nicotinic acetylcholine receptors. J Biol Chem **277**, 33610-33615

30. Nicke, A., Loughnan, M. L., Millard, E. L., Alewood, P. F., Adams, D. J., Daly, N. L., Craik, D. J., and Lewis, R. J. (2003) Isolation, structure, and activity of GID, a novel alpha 4/7-conotoxin with an extended N-terminal sequence. J Biol Chem **278**, 3137-3144

31. Talley, T. T., Olivera, B. M., Han, K. H., Christensen, S. B., Dowell, C., Tsigelny, I., Ho, K. Y., Taylor, P., and McIntosh, J. M. (2006) Alpha-conotoxin OmIA is a potent ligand for the acetylcholine-binding protein as well as alpha3beta2 and alpha7 nicotinic acetylcholine receptors. J Biol Chem **281**, 24678-24686

32. McIntosh, J. M., Plazas, P. V., Watkins, M., Gomez-Casati, M. E., Olivera, B. M., and Elgoyhen, A. B. (2005) A novel alpha-conotoxin, PeIA, cloned from Conus pergrandis, discriminates between rat alpha9alpha10 and alpha7 nicotinic cholinergic receptors. J Biol Chem **280**, 30107-30112

33. Dowell, C., Olivera, B. M., Garrett, J. E., Staheli, S. T., Watkins, M., Kuryatov, A., Yoshikami, D., Lindstrom, J. M., and McIntosh, J. M. (2003) Alpha-conotoxin PIA is selective for alpha6 subunit-containing nicotinic acetylcholine receptors. J Neurosci **23**, 8445-8452

34. Fainzilber, M., Hasson, A., Oren, R., Burlingame, A. L., Gordon, D., Spira, M. E., and Zlotkin, E. (1994) New mollusc-specific alpha-conotoxins block Aplysia neuronal acetylcholine receptors. Biochemistry **33**, 9523-9529

35. Lopez-Vera, E., Aguilar, M. B., Schiavon, E., Marinzi, C., Ortiz, E., Restano Cassulini, R., Batista, C. V., Possani, L. D., Heimer de la Cotera, E. P., Peri, F., Becerril, B., and Wanke, E. (2007) Novel alpha-conotoxins from Conus spurius and the alpha-conotoxin EI share high-affinity potentiation and low-affinity inhibition of nicotinic acetylcholine receptors. FEBS J **274**, 3972-3985

36. Sandall, D. W., Satkunanathan, N., Keays, D. A., Polidano, M. A., Liping, X., Pham, V., Down, J. G., Khalil, Z., Livett, B. G., and Gayler, K. R. (2003) A novel alpha-conotoxin identified by gene sequencing is active in suppressing the vascular response to selective stimulation of sensory nerves in vivo. Biochemistry **42**, 6904-6911

37. Peng, C., Han, Y., Sanders, T., Chew, G., Liu, J., Hawrot, E., Chi, C., and Wang, C. (2008) alpha4/7-conotoxin Lp1.1 is a novel antagonist of neuronal nicotinic acetylcholine receptors. Peptides **29**, 1700-1707

38. Santos, A. D., McIntosh, J. M., Hillyard, D. R., Cruz, L. J., and Olivera, B. M. (2004) The A-superfamily of conotoxins: structural and functional divergence. J Biol Chem **279**, 17596-17606

39. Lopez-Vera, E., Jacobsen, R. B., Ellison, M., Olivera, B. M., and Teichert, R. W. (2007) A novel alpha conotoxin (alpha-PIB) isolated from C. purpurascens is selective for skeletal muscle nicotinic acetylcholine receptors. Toxicon **49**, 1193-1199

40. Ellison, M., McIntosh, J. M., and Olivera, B. M. (2003) Alpha-conotoxins ImI and ImII. Similar alpha 7 nicotinic receptor antagonists act at different sites. J Biol Chem **278**, 757-764

41. Favreau, P., Krimm, I., Le Gall, F., Bobenrieth, M. J., Lamthanh, H., Bouet, F., Servent, D., Molgo, J., Menez, A., Letourneux, Y., and Lancelin, J. M. (1999) Biochemical characterization and nuclear magnetic resonance structure of novel alpha-conotoxins isolated from the venom of Conus consors. Biochemistry **38**, 6317-6326

42. Gray, W. R., Luque, A., Olivera, B. M., Barrett, J., and Cruz, L. J. (1981) Peptide toxins from Conus geographus venom. J Biol Chem **256**, 4734-4740

43. Tsetlin, V., Utkin, Y., and Kasheverov, I. (2009) Polypeptide and peptide toxins, magnifying lenses for binding sites in nicotinic acetylcholine receptors. Biochem Pharmacol **78**, 720-731

44. Dutertre, S., and Lewis, R. J. (2006) Toxin insights into nicotinic acetylcholine receptors. Biochem Pharmacol **72**, 661-670

45. Quiram, P. A., Jones, J. J., and Sine, S. M. (1999) Pairwise interactions between neuronal α7 acetylcholine receptors and α-conotoxin ImI. J. Biol. Chem. **274**, 19517-19524

46. Quiram, P. A., McIntosh, J. M., and Sine, S. M. (2000) Pairwise interactions between neuronal alpha(7) acetylcholine receptors and alpha-conotoxin PnIB. J Biol Chem **275**, 4889-4896

47. Azam, L., Maskos, U., Changeux, J. P., Dowell, C. D., Christensen, S., De Biasi, M., and McIntosh, J. M. (2010) alpha-Conotoxin BuIA[T5A;P6O]: a novel ligand that discriminates between alpha6ss4 and alpha6ss2 nicotinic acetylcholine receptors and blocks nicotine-stimulated norepinephrine release. Faseb J **24**, 5113-5123

48. Skok, V. I. (2002) Nicotinic acetylcholine receptors in autonomic ganglia. Auton Neurosci **97**, 1-11

49. Wang, N., Orr-Urtreger, A., and Korczyn, A. D. (2002) The role of neuronal nicotinic acetylcholine receptor subunits in autonomic ganglia: lessons from knockout mice. Prog Neurobiol **68**, 341-360

50. Kuffler, S. W., and Yoshikami, D. (1975) The number of transmitter molecules in a quantum: an estimate from iontophoretic application of acetylcholine at the neuromuscular synapse. J Physiol **251**, 465-482

51. Kuffler, S. W., and Yoshikami, D. (1975) The distribution of acetylcholine sensitivity at the post-synaptic membrane of vertebrate skeletal twitch muscles: iontophoretic mapping in the micron range. J Physiol **244**, 703-730

52. Marchi, M., and Grilli, M. (2010) Presynaptic nicotinic receptors modulating neurotransmitter release in the central nervous system: functional interactions with other coexisting receptors. Prog Neurobiol **92**, 105-111

53. Robinson, L., Platt, B., and Riedel, G. (2011) Involvement of the cholinergic system in conditioning and perceptual memory. Behav Brain Res **221**, 443-465

54. Levin, E. D. (2012) alpha7-Nicotinic receptors and cognition. Curr Drug Targets **13**, 602-606

55. Quik, M., and McIntosh, J. M. (2006) Striatal alpha6* nicotinic acetylcholine receptors: potential targets for Parkinson's disease therapy. J Pharmacol Exp Ther **316**, 481-489

56. Parri, H. R., Hernandez, C. M., and Dineley, K. T. (2011) Research update: Alpha7 nicotinic acetylcholine receptor mechanisms in Alzheimer's disease. Biochem Pharmacol **82**, 931-942

57. Dani, J. A., Jenson, D., Broussard, J. I., and De Biasi, M. (2011) Neurophysiology of nicotine addiction. J Addict Res Ther **S1**

58. De Biasi, M., and Dani, J. A. (2011) Reward, addiction, withdrawal to nicotine. Annu Rev Neurosci **34**, 105-130

59. Leonard, S., Gault, J., Hopkins, J., Logel, J., Vianzon, R., Short, M., Drebing, C., Berger, R., Venn, D., Sirota, P., Zerbe, G., Olincy, A., Ross, R. G., Adler, L. E., and Freedman, R. (2002) Association of promoter variants in the alpha7 nicotinic acetylcholine receptor subunit gene with an inhibitory deficit found in schizophrenia. Arch Gen Psychiatry **59**, 1085-1096

60. Leonard, S., and Freedman, R. (2006) Genetics of chromosome 15q13-q14 in schizophrenia. Biol Psychiatry **60**, 115-122

61. Millar, N. S., and Gotti, C. (2009) Diversity of vertebrate nicotinic acetylcholine receptors. Neuropharmacology **56**, 237-246

62. Elgoyhen, A. B., Johnson, D. S., Boulter, J., Vetter, D. E., and Heinemann, S. (1994) Alpha 9: an acetylcholine receptor with novel pharmacological properties expressed in rat cochlear hair cells. Cell **79**, 705-715

63. Lips, K. S., Pfeil, U., and Kummer, W. (2002) Coexpression of alpha 9 and alpha 10 nicotinic acetylcholine receptors in rat dorsal root ganglion neurons. Neuroscience **115**, 1-5

64. Lips, K. S., Bruggmann, D., Pfeil, U., Vollerthun, R., Grando, S. A., and Kummer, W. (2005) Nicotinic acetylcholine receptors in rat and human placenta. Placenta **26**, 735-746

65. Kummer, W., Lips, K. S., and Pfeil, U. (2008) The epithelial cholinergic system of the airways. Histochem Cell Biol **130**, 219-234

66. Colomer, C., Olivos-Ore, L. A., Vincent, A., McIntosh, J. M., Artalejo, A. R., and Guerineau, N. C. (2010) Functional characterization of alpha9-containing cholinergic nicotinic receptors in the rat adrenal medulla: implication in stress-induced functional plasticity. J Neurosci **30**, 6732-6742

67. Verbitsky, M., Rothlin, C. V., Katz, E., and Elgoyhen, A. B. (2000) Mixed nicotinic-muscarinic properties of the alpha9 nicotinic cholinergic receptor. Neuropharmacology **39**, 2515-2524

68. Sgard, F., Charpantier, E., Bertrand, S., Walker, N., Caput, D., Graham, D., Bertrand, D., and Besnard, F. (2002) A novel human nicotinic receptor subunit, alpha10, that confers functionality to the alpha9-subunit. Mol Pharmacol **61**, 150-159

69. Vincler, M. (2005) Neuronal nicotinic receptors as targets for novel analgesics. Expert Opin Investig Drugs **14**, 1191-1198

70. Vincler, M., Wittenauer, S., Parker, R., Ellison, M., Olivera, B. M., and McIntosh, J. M. (2006) Molecular mechanism for analgesia involving specific antagonism of alpha9alpha10 nicotinic acetylcholine receptors. Proc Natl Acad Sci U S A **103**, 17880-17884

71. Vincler, M., and McIntosh, J. M. (2007) Targeting the alpha9alpha10 nicotinic acetylcholine receptor to treat severe pain. Expert Opin Ther Targets **11**, 891-897

72. McIntosh, J. M., Absalom, N., Chebib, M., Elgoyhen, A. B., and Vincler, M. (2009) Alpha9 nicotinic acetylcholine receptors and the treatment of pain. Biochem Pharmacol **78**, 693-702

73. Holtman, J. R., Dwoskin, L. P., Dowell, C., Wala, E. P., Zhang, Z., Crooks, P. A., and McIntosh, J. M. (2011) The novel small molecule alpha9alpha10 nicotinic acetylcholine receptor antagonist ZZ-204G is analgesic. Eur J Pharmacol **670**, 500-508

74. Wala, E. P., Crooks, P. A., McIntosh, J. M., and Holtman, J. R., Jr. (2012) Novel small molecule alpha9alpha10 nicotinic receptor antagonist prevents and reverses chemotherapy-evoked neuropathic pain in rats. Anesth Analg **115**, 713-720

75. Nguyen, V. T., Ndoye, A., and Grando, S. A. (2000) Novel human alpha9 acetylcholine receptor regulating keratinocyte adhesion is targeted by Pemphigus vulgaris autoimmunity. Am J Pathol **157**, 1377-1391

76. Vetter, D. E., Liberman, M. C., Mann, J., Barhanin, J., Boulter, J., Brown, M. C., Saffiote-Kolman, J., Heinemann, S. F., and Elgoyhen, A. B. (1999) Role of alpha9 nicotinic ACh receptor subunits in the development and function of cochlear efferent innervation. Neuron **23**, 93-103

77. Maison, S. F., Luebke, A. E., Liberman, M. C., and Zuo, J. (2002) Efferent protection from acoustic injury is mediated via alpha9 nicotinic acetylcholine receptors on outer hair cells. J Neurosci **22**, 10838-10846

78. Elgoyhen, A. B., Vetter, D. E., Katz, E., Rothlin, C. V., Heinemann, S. F., and Boulter, J. (2001) alpha10: a determinant of nicotinic cholinergic receptor

function in mammalian vestibular and cochlear mechanosensory hair cells. Proc Natl Acad Sci U S A **98**, 3501-3506

79. Lustig, L. R., Peng, H., Hiel, H., Yamamoto, T., and Fuchs, P. A. (2001) Molecular cloning and mapping of the human nicotinic acetylcholine receptor alpha10 (CHRNA10). Genomics **73**, 272-283

80. Gopalakrishnan, M., Monteggia, L. M., Anderson, D. J., Molinari, E. J., Piattoni-Kaplan, M., Donnelly-Roberts, D., Arneric, S. P., and Sullivan, J. P. (1996) Stable expression, pharmacologic properties and regulation of the human neuronal nicotinic acetylcholine alpha 4 beta 2 receptor. J Pharmacol Exp Ther **276**, 289-297

81. Eaton, J. B., Peng, J. H., Schroeder, K. M., George, A. A., Fryer, J. D., Krishnan, C., Buhlman, L., Kuo, Y. P., Steinlein, O., and Lukas, R. J. (2003) Characterization of human alpha 4 beta 2-nicotinic acetylcholine receptors stably and heterologously expressed in native nicotinic receptor-null SH-EP1 human epithelial cells. Mol Pharmacol **64**, 1283-1294

82. Deneris, E. S., Connolly, J., Boulter, J., Wada, E., Wada, K., Swanson, L. W., Patrick, J., and Heinemann, S. (1988) Primary structure and expression of beta 2: a novel subunit of neuronal nicotinic acetylcholine receptors. Neuron **1**, 45-54

83. Couturier, S., Bertrand, D., Matter, J. M., Hernandez, M. C., Bertrand, S., Millar, N., Valera, S., Barkas, T., and Ballivet, M. (1990) A neuronal nicotinic acetylcholine receptor subunit (alpha 7) is developmentally regulated and forms a homo-oligomeric channel blocked by alpha-BTX. Neuron **5**, 847-856

84. Gotti, C., Hanke, W., Maury, K., Moretti, M., Ballivet, M., Clementi, F., and Bertrand, D. (1994) Pharmacology and biophysical properties of alpha 7 and alpha 7-alpha 8 alpha-bungarotoxin receptor subtypes immunopurified from the chick optic lobe. Eur J Neurosci **6**, 1281-1291

85. van Kleef, R. G., Vijverberg, H. P., and Westerink, R. H. (2008) Selective inhibition of human heteromeric alpha9alpha10 nicotinic acetylcholine receptors at a low agonist concentration by low concentrations of ototoxic organic solvents. Toxicol In Vitro **22**, 1568-1572

86. Halai, R., Clark, R. J., Nevin, S. T., Jensen, J. E., Adams, D. J., and Craik, D. J. (2009) Scanning mutagenesis of alpha-conotoxin Vc1.1 reveals residues crucial for activity at the alpha9alpha10 nicotinic acetylcholine receptor. J Biol Chem **284**, 20275-20284

87. Lansdell, S. J., Gee, V. J., Harkness, P. C., Doward, A. I., Baker, E. R., Gibb, A. J., and Millar, N. S. (2005) RIC-3 enhances functional expression of multiple nicotinic acetylcholine receptor subtypes in mammalian cells. Mol Pharmacol **68**, 1431-1438

88. Fucile, S., Sucapane, A., and Eusebi, F. (2006) Ca2+ permeability through rat cloned alpha9-containing nicotinic acetylcholine receptors. Cell Calcium **39**, 349-355

89. Gray, N. K., and Hentze, M. W. (1994) Regulation of protein synthesis by mRNA structure. Mol Biol Rep **19**, 195-200

90. Jacobs, E., Mills, J. D., and Janitz, M. (2012) The role of RNA structure in posttranscriptional regulation of gene expression. J Genet Genomics **39**, 535-543

91. Kozak, M. (2005) Regulation of translation via mRNA structure in prokaryotes and eukaryotes. Gene **361**, 13-37

92. Nomura, M., Ohsuye, K., Mizuno, A., Sakuragawa, Y., and Tanaka, S. (1984) Influence of messenger RNA secondary structure on translation efficiency. Nucleic Acids Symp Ser, 173-176

93. Kozak, M. (1990) Downstream secondary structure facilitates recognition of initiator codons by eukaryotic ribosomes. Proc Natl Acad Sci U S A **87**, 8301-8305

94. Pesole, G., Grillo, G., Larizza, A., and Liuni, S. (2000) The untranslated regions of eukaryotic mRNAs: structure, function, evolution and bioinformatic tools for their analysis. Brief Bioinform **1**, 236-249

95. Araujo, P. R., Yoon, K., Ko, D., Smith, A. D., Qiao, M., Suresh, U., Burns, S. C., and Penalva, L. O. (2012) Before it gets started: regulating translation at the 5' UTR. Comp Funct Genomics **2012**, 475731

96. Wilkie, G. S., Dickson, K. S., and Gray, N. K. (2003) Regulation of mRNA translation by 5'- and 3'-UTR-binding factors. Trends Biochem Sci **28**, 182-188

97. Falcone, D., and Andrews, D. W. (1991) Both the 5' untranslated region and the sequences surrounding the start site contribute to efficient initiation of translation in vitro. Mol Cell Biol **11**, 2656-2664

98. Liman, E. R., Tytgat, J., and Hess, P. (1992) Subunit stoichiometry of a mammalian K+ channel determined by construction of multimeric cDNAs. Neuron **9**, 861-871

99. Kruys, V., Wathelet, M., Poupart, P., Contreras, R., Fiers, W., Content, J., and Huez, G. (1987) The 3' untranslated region of the human interferon-beta mRNA has an inhibitory effect on translation. Proceedings of the National Academy of Sciences of the United States of America **84**, 6030-6034

100. Kariko, K., Kuo, A., and Barnathan, E. (1999) Overexpression of urokinase receptor in mammalian cells following administration of the in vitro transcribed encoding mRNA. Gene Ther **6**, 1092-1100

101. Fan, Q., Treder, K., and Miller, W. A. (2012) Untranslated regions of diverse plant viral RNAs vary greatly in translation enhancement efficiency. BMC Biotechnol **12**, 22

102. Gallie, D. R., Sleat, D. E., Watts, J. W., Turner, P. C., and Wilson, T. M. (1987) The 5'-leader sequence of tobacco mosaic virus RNA enhances the expression of foreign gene transcripts in vitro and in vivo. Nucleic Acids Res **15**, 3257-3273

103. Gallie, D. R., and Walbot, V. (1992) Identification of the motifs within the tobacco mosaic virus 5'-leader responsible for enhancing translation. Nucleic Acids Res **20**, 4631-4638

104. Gallie, D. R., Sleat, D. E., Watts, J. W., Turner, P. C., and Wilson, T. M. (1987) A comparison of eukaryotic viral 5'-leader sequences as enhancers of mRNA expression in vivo. Nucleic Acids Res **15**, 8693-8711

105. Jobling, S. A., and Gehrke, L. (1987) Enhanced translation of chimaeric messenger RNAs containing a plant viral untranslated leader sequence. Nature **325**, 622-625

106. Sleat, D. E., Gallie, D. R., Jefferson, R. A., Bevan, M. W., Turner, P. C., and Wilson, T. M. (1987) Characterisation of the 5'-leader sequence of tobacco mosaic virus RNA as a general enhancer of translation in vitro. Gene **60**, 217-225

107. Sumikawa, K., Houghton, M., Emtage, J. S., Richards, B. M., and Barnard, E. A. (1981) Active multi-subunit ACh receptor assembled by translation of heterologous mRNA in Xenopus oocytes. Nature **292**, 862-864

108. Barnard, E. A., Miledi, R., and Sumikawa, K. (1982) Translation of exogenous messenger RNA coding for nicotinic acetylcholine receptors produces functional receptors in Xenopus oocytes. Proc R Soc Lond B Biol Sci **215**, 241-246

109. Papke, R. L., Boulter, J., Patrick, J., and Heinemann, S. (1989) Single-channel currents of rat neuronal nicotinic acetylcholine receptors expressed in Xenopus oocytes. Neuron **3**, 589-596

110. Duvoisin, R. M., Deneris, E. S., Patrick, J., and Heinemann, S. (1989) The functional diversity of the neuronal nicotinic acetylcholine receptors is increased by a novel subunit: beta 4. Neuron **3**, 487-496

111. Kuryatov, A., Olale, F., Cooper, J., Choi, C., and Lindstrom, J. (2000) Human alpha6 AChR subtypes: subunit composition, assembly, and pharmacological responses. Neuropharmacology **39**, 2570-2590

112. Kozak, M. (1986) Point mutations define a sequence flanking the AUG initiator codon that modulates translation by eukaryotic ribosomes. Cell **44**, 283-292

113. Soreq, H., Ben-Aziz, R., Prody, C. A., Seidman, S., Gnatt, A., Neville, L., Lieman-Hurwitz, J., Lev-Lehman, E., Ginzberg, D., Lipidot-Lifson, Y., and et al. (1990) Molecular cloning and construction of the coding region for human acetylcholinesterase reveals a G + C-rich attenuating structure. Proc Natl Acad Sci U S A **87**, 9688-9692

114. Morel, N., and Massoulie, J. (2000) Comparative expression of homologous proteins. A novel mode of transcriptional regulation by the coding sequence folding compatibility of chimeras. J Biol Chem **275**, 7304-7312

115. Lammich, S., Schobel, S., Zimmer, A. K., Lichtenthaler, S. F., and Haass, C. (2004) Expression of the Alzheimer protease BACE1 is suppressed via its 5'-untranslated region. EMBO Rep **5**, 620-625

116. Niesler, B., Flohr, T., Nothen, M. M., Fischer, C., Rietschel, M., Franzek, E., Albus, M., Propping, P., and Rappold, G. A. (2001) Association between the 5' UTR variant C178T of the serotonin receptor gene HTR3A and bipolar affective disorder. Pharmacogenetics **11**, 471-475

117. Mihailovich, M., Thermann, R., Grohovaz, F., Hentze, M. W., and Zacchetti, D. (2007) Complex translational regulation of BACE1 involves upstream AUGs and stimulatory elements within the 5' untranslated region. Nucleic Acids Res **35**, 2975-2985

118. Venkatachalan, S. P., Bushman, J. D., Mercado, J. L., Sancar, F., Christopherson, K. R., and Boileau, A. J. (2007) Optimized expression vector for ion channel studies in Xenopus oocytes and mammalian cells using alfalfa mosaic virus. Pflugers Arch **454**, 155-163

119. Gallie, D. R. (2002) The 5'-leader of tobacco mosaic virus promotes translation through enhanced recruitment of eIF4F. Nucleic Acids Res **30**, 3401-3411

120. Brederode, F. T., Koper-Zwarthoff, E. C., and Bol, J. F. (1980) Complete nucleotide sequence of alfalfa mosaic virus RNA 4. Nucleic Acids Res **8**, 2213-2223

121. Gehrke, L., Auron, P. E., Quigley, G. J., Rich, A., and Sonenberg, N. (1983) 5'-Conformation of capped alfalfa mosaic virus ribonucleic acid 4 may reflect its independence of the cap structure or of cap-binding protein for efficient translation. Biochemistry **22**, 5157-5164

122. Chatterjee, S., and Pal, J. K. (2009) Role of 5'- and 3'-untranslated regions of mRNAs in human diseases. Biol Cell **101**, 251-262

123. Hudder, A., and Werner, R. (2000) Analysis of a Charcot-Marie-Tooth disease mutation reveals an essential internal ribosome entry site element in the connexin-32 gene. J Biol Chem **275**, 34586-34591

124. Brown, C. Y., Mize, G. J., Pineda, M., George, D. L., and Morris, D. R. (1999) Role of two upstream open reading frames in the translational control of oncogene mdm2. Oncogene **18**, 5631-5637

125. Jin, X., Turcott, E., Englehardt, S., Mize, G. J., and Morris, D. R. (2003) The two upstream open reading frames of oncogene mdm2 have different translational regulatory properties. J Biol Chem **278**, 25716-25721

126. Morris, D. R., and Geballe, A. P. (2000) Upstream open reading frames as regulators of mRNA translation. Molecular and Cellular Biology **20**, 8635-8642

127. Soreq, H., Nudel, U., Salomon, R., Revel, M., and Littauer, U. Z. (1974) In vitro translation of polyadenylic acid-free rabbit globin messenger RNA. J Mol Biol **88**, 233-245

128. Huez, G., Marbaix, G., Hubert, E., Leclercq, M., Nudel, U., Soreq, H., Salomon, R., Lebleu, B., Revel, M., and Littauer, U. Z. (1974) Role of the polyadenylate segment in the translation of globin messenger RNA in Xenopus oocytes. Proc Natl Acad Sci U S A **71**, 3143-3146

129. Pascale, A., and Govoni, S. (2012) The complex world of post-transcriptional mechanisms: is their deregulation a common link for diseases? Focus on ELAV-like RNA-binding proteins. Cell Mol Life Sci **69**, 501-517

130. Alexander, J. K., Govind, A. P., Drisdel, R. C., Blanton, M. P., Vallejo, Y., Lam, T. T., and Green, W. N. (2010) Palmitoylation of nicotinic acetylcholine receptors. J Mol Neurosci **40**, 12-20

131. Swope, S. L., Moss, S. J., Raymond, L. A., and Huganir, R. L. (1999) Regulation of ligand-gated ion channels by protein phosphorylation. Adv Second Messenger Phosphoprotein Res **33**, 49-78

132. daCosta, C. J., Kaiser, D. E., and Baenziger, J. E. (2005) Role of glycosylation and membrane environment in nicotinic acetylcholine receptor stability. Biophys J **88**, 1755-1764

133. Nishizaki, T. (2003) N-glycosylation sites on the nicotinic ACh receptor subunits regulate receptor channel desensitization and conductance. Brain Res Mol Brain Res **114**, 172-176

134. Chang, W., Gelman, M. S., and Prives, J. M. (1997) Calnexin-dependent enhancement of nicotinic acetylcholine receptor assembly and surface expression. J Biol Chem **272**, 28925-28932

135. Wanamaker, C. P., and Green, W. N. (2007) Endoplasmic reticulum chaperones stabilize nicotinic receptor subunits and regulate receptor assembly. J Biol Chem **282**, 31113-31123

136. Srinivasan, R., Pantoja, R., Moss, F. J., Mackey, E. D., Son, C. D., Miwa, J., and Lester, H. A. (2011) Nicotine up-regulates alpha4beta2 nicotinic receptors and ER exit sites via stoichiometry-dependent chaperoning. J Gen Physiol **137**, 59-79

137. Lester, H. A., Xiao, C., Srinivasan, R., Son, C. D., Miwa, J., Pantoja, R., Banghart, M. R., Dougherty, D. A., Goate, A. M., and Wang, J. C. (2009) Nicotine is a selective pharmacological chaperone of acetylcholine receptor number and stoichiometry. Implications for drug discovery. AAPS J **11**, 167-177

138. Kuryatov, A., Luo, J., Cooper, J., and Lindstrom, J. (2005) Nicotine acts as a pharmacological chaperone to up-regulate human alpha4beta2 acetylcholine receptors. Mol Pharmacol **68**, 1839-1851

139. Valles, A. S., and Barrantes, F. J. (2012) Chaperoning alpha7 neuronal nicotinic acetylcholine receptors. Biochim Biophys Acta **1818**, 718-729

140. Valles, A. S., Roccamo, A. M., and Barrantes, F. J. (2009) Ric-3 chaperone-mediated stable cell-surface expression of the neuronal alpha7 nicotinic acetylcholine receptor in mammalian cells. Acta Pharmacol Sin **30**, 818-827

141. Williams, M. E., Burton, B., Urrutia, A., Shcherbatko, A., Chavez-Noriega, L. E., Cohen, C. J., and Aiyar, J. (2005) Ric-3 promotes functional expression of the nicotinic acetylcholine receptor alpha7 subunit in mammalian cells. J Biol Chem **280**, 1257-1263

142. Roncarati, R., Seredenina, T., Jow, B., Jow, F., Papini, S., Kramer, A., Bothmann, H., Dunlop, J., and Terstappen, G. C. (2008) Functional properties of alpha7 nicotinic acetylcholine receptors co-expressed with RIC-3 in a stable recombinant CHO-K1 cell line. Assay Drug Dev Technol **6**, 181-193

143. Cheng, A., McDonald, N. A., and Connolly, C. N. (2005) Cell surface expression of 5-hydroxytryptamine type 3 receptors is promoted by RIC-3. J Biol Chem **280**, 22502-22507

144. Nie, L., Song, H., Chen, M. F., Chiamvimonvat, N., Beisel, K. W., Yamoah, E. N., and Vazquez, A. E. (2004) Cloning and expression of a small-conductance Ca(2+)-activated K+ channel from the mouse cochlea: coexpression with alpha9/alpha10 acetylcholine receptors. J Neurophysiol **91**, 1536-1544

145. Baker, E. R., Zwart, R., Sher, E., and Millar, N. S. (2004) Pharmacological properties of alpha 9 alpha 10 nicotinic acetylcholine receptors revealed by heterologous expression of subunit chimeras. Mol Pharmacol **65**, 453-460

146. Osman, A. A., Schrader, A. D., Hawkes, A. J., Akil, O., Bergeron, A., Lustig, L. R., and Simmons, D. D. (2008) Muscle-like nicotinic receptor accessory molecules in sensory hair cells of the inner ear. Mol Cell Neurosci **38**, 153-169

147. Flores, C. M., Rogers, S. W., Pabreza, L. A., Wolfe, B. B., and Kellar, K. J. (1992) A subtype of nicotinic cholinergic receptor in rat brain is composed of alpha 4 and beta 2 subunits and is up-regulated by chronic nicotine treatment. Mol Pharmacol **41**, 31-37

148. Lee, C. H., Huang, C. S., Chen, C. S., Tu, S. H., Wang, Y. J., Chang, Y. J., Tam, K. W., Wei, P. L., Cheng, T. C., Chu, J. S., Chen, L. C., Wu, C. H., and Ho, Y. S. (2010) Overexpression and activation of the alpha9-nicotinic receptor during tumorigenesis in human breast epithelial cells. J Natl Cancer Inst **102**, 1322-1335

149. McKay, B. E., Placzek, A. N., and Dani, J. A. (2007) Regulation of synaptic transmission and plasticity by neuronal nicotinic acetylcholine receptors. Biochem Pharmacol **74**, 1120-1133

150. Wonnacott, S. (1997) Presynaptic nicotinic ACh receptors. Trends Neurosci **20**, 92-98

151. Vizi, E. S., and Lendvai, B. (1999) Modulatory role of presynaptic nicotinic receptors in synaptic and non-synaptic chemical communication in the central nervous system. Brain Res Brain Res Rev **30**, 219-235

152. MacDermott, A. B., Role, L. W., and Siegelbaum, S. A. (1999) Presynaptic ionotropic receptors and the control of transmitter release. Annu Rev Neurosci **22**, 443-485

153. Diaz-Hernandez, M., Pintor, J., Castro, E., and Miras-Portugal, M. T. (2002) Co-localisation of functional nicotinic and ionotropic nucleotide receptors in isolated cholinergic synaptic terminals. Neuropharmacology **42**, 20-33

154. Jiang, L. H., Kim, M., Spelta, V., Bo, X., Surprenant, A., and North, R. A. (2003) Subunit arrangement in P2X receptors. J Neurosci **23**, 8903-8910

155. North, R. A. (2002) Molecular physiology of P2X receptors. Physiol Rev **82**, 1013-1067

156. Murrell-Lagnado, R. D., and Qureshi, O. S. (2008) Assembly and trafficking of P2X purinergic receptors (Review). Mol Membr Biol **25**, 321-331

157. Shi, L., Zhang, H. H., Hu, J., Jiang, X. H., and Xu, G. Y. (2012) Purinergic P2X receptors and diabetic neuropathic pain. Sheng Li Xue Bao **64**, 531-542

158. Jacob, F., Novo, C. P., Bachert, C., and Van Crombruggen, K. (2013) Purinergic signaling in inflammatory cells: P2 receptor expression, functional effects, and modulation of inflammatory responses. Purinergic Signal 2013, Feb 13

159. Trang, T., and Salter, M. W. (2012) P2X4 purinoceptor signaling in chronic pain. Purinergic Signal **8**, 621-628

160. Ferrero, M. E. (2011) Purinoceptors in inflammation: potential as anti-inflammatory therapeutic targets. Front Biosci **16**, 2172-2186

161. Deli, T., and Csernoch, L. (2008) Extracellular ATP and cancer: an overview with special reference to P2 purinergic receptors. Pathol Oncol Res **14**, 219-231

162. Decker, D. A., and Galligan, J. J. (2009) Cross-inhibition between nicotinic acetylcholine receptors and P2X receptors in myenteric neurons and HEK-293 cells. Am J Physiol Gastrointest Liver Physiol **296**, G1267-1276

163. Khakh, B. S., Zhou, X., Sydes, J., Galligan, J. J., and Lester, H. A. (2000) State-dependent cross-inhibition between transmitter-gated cation channels. Nature **406**, 405-410

164. Decker, D. A., and Galligan, J. J. (2010) Molecular mechanisms of cross-inhibition between nicotinic acetylcholine receptors and P2X receptors in myenteric neurons and HEK-293 cells. Neurogastroenterol Motil **22**, 901-908, e235

165. Barajas-Lopez, C., Espinosa-Luna, R., and Zhu, Y. (1998) Functional interactions between nicotinic and P2X channels in short-term cultures of guinea-pig submucosal neurons. J Physiol **513 (Pt 3)**, 671-683

166. Rodrigues, R. J., Almeida, T., de Mendonca, A., and Cunha, R. A. (2006) Interaction between P2X and nicotinic acetylcholine receptors in glutamate nerve terminals of the rat hippocampus. J Mol Neurosci **30**, 173-176

167. Elgoyhen, A. B., and Katz, E. (2012) The efferent medial olivocochlear-hair cell synapse. J Physiol Paris **106**, 47-56

168. Szucs, A., Szappanos, H., Toth, A., Farkas, Z., Panyi, G., Csernoch, L., and Sziklai, I. (2004) Differential expression of purinergic receptor subtypes in the outer hair cells of the guinea pig. Hear Res **196**, 2-7

169. Wikstrom, M. A., Lawoko, G., and Heilbronn, E. (1998) Cholinergic modulation of extracellular ATP-induced cytoplasmic calcium concentrations in cochlear outer hair cells. J Physiol Paris **92**, 345-349

170. Kawashima, K., Yoshikawa, K., Fujii, Y. X., Moriwaki, Y., and Misawa, H. (2007) Expression and function of genes encoding cholinergic components in murine immune cells. Life Sci **80**, 2314-2319

171. Peng, H., Ferris, R. L., Matthews, T., Hiel, H., Lopez-Albaitero, A., and Lustig, L. R. (2004) Characterization of the human nicotinic acetylcholine receptor subunit alpha (alpha) 9 (CHRNA9) and alpha (alpha) 10 (CHRNA10) in lymphocytes. Life Sci **76**, 263-280

172. Tracey, K. J. (2009) Reflex control of immunity. Nat Rev Immunol **9**, 418-428

173. Wang, H., Yu, M., Ochani, M., Amella, C. A., Tanovic, M., Susarla, S., Li, J. H., Yang, H., Ulloa, L., Al-Abed, Y., Czura, C. J., and Tracey, K. J. (2003) Nicotinic acetylcholine receptor alpha7 subunit is an essential regulator of inflammation. Nature **421**, 384-388

174. Simard, A. R., Gan, Y., St-Pierre, S., Kousari, A., Patel, V., Whiteaker, P., Morley, B. J., Lukas, R. J., and Shi, F. D. (2013) Differential modulation of EAE by alpha9*- and beta2*-nicotinic acetylcholine receptors. Immunol Cell Biol **91**, 195-200

175. Rayah, A., Kanellopoulos, J. M., and Di Virgilio, F. (2012) P2 receptors and immunity. Microbes Infect **14**, 1254-1262

176. Di Virgilio, F., Chiozzi, P., Ferrari, D., Falzoni, S., Sanz, J. M., Morelli, A., Torboli, M., Bolognesi, G., and Baricordi, O. R. (2001) Nucleotide receptors: an emerging family of regulatory molecules in blood cells. Blood **97**, 587-600

177. Ferrari, D., Chiozzi, P., Falzoni, S., Dal Susino, M., Melchiorri, L., Baricordi, O. R., and Di Virgilio, F. (1997) Extracellular ATP triggers IL-1 beta release by activating the purinergic P2Z receptor of human macrophages. J Immunol **159**, 1451-1458

178. Chessell, I. P., Hatcher, J. P., Bountra, C., Michel, A. D., Hughes, J. P., Green, P., Egerton, J., Murfin, M., Richardson, J., Peck, W. L., Grahames, C. B., Casula, M. A., Yiangou, Y., Birch, R., Anand, P., and Buell, G. N. (2005) Disruption of the P2X7 purinoceptor gene abolishes chronic inflammatory and neuropathic pain. Pain **114**, 386-396

179. Solle, M., Labasi, J., Perregaux, D. G., Stam, E., Petrushova, N., Koller, B. H., Griffiths, R. J., and Gabel, C. A. (2001) Altered cytokine production in mice lacking P2X(7) receptors. J Biol Chem **276**, 125-132

180. Labasi, J. M., Petrushova, N., Donovan, C., McCurdy, S., Lira, P., Payette, M. M., Brissette, W., Wicks, J. R., Audoly, L., and Gabel, C. A. (2002) Absence of the P2X7 receptor alters leukocyte function and attenuates an inflammatory response. J Immunol **168**, 6436-6445

181. Sharp, A. J., Polak, P. E., Simonini, V., Lin, S. X., Richardson, J. C., Bongarzone, E. R., and Feinstein, D. L. (2008) P2x7 deficiency suppresses development of experimental autoimmune encephalomyelitis. J Neuroinflammation **5**, 33

182. Chen, L., and Brosnan, C. F. (2006) Exacerbation of experimental autoimmune encephalomyelitis in P2X7R-/- mice: evidence for loss of apoptotic activity in lymphocytes. J Immunol **176**, 3115-3126

183. Bours, M. J., Dagnelie, P. C., Giuliani, A. L., Wesselius, A., and Di Virgilio, F. (2011) P2 receptors and extracellular ATP: a novel homeostatic pathway in inflammation. Front Biosci (Schol Ed) **3**, 1443-1456

184. Ulmann, L., Hirbec, H., and Rassendren, F. (2010) P2X4 receptors mediate PGE2 release by tissue-resident macrophages and initiate inflammatory pain. EMBO J **29**, 2290-2300

185. Tsuda, M., Kuboyama, K., Inoue, T., Nagata, K., Tozaki-Saitoh, H., and Inoue, K. (2009) Behavioral phenotypes of mice lacking purinergic P2X4 receptors in acute and chronic pain assays. Mol Pain **5**, 28

186. Soto, F., Garcia-Guzman, M., Gomez-Hernandez, J. M., Hollmann, M., Karschin, C., and Stuhmer, W. (1996) P2X4: an ATP-activated ionotropic receptor cloned from rat brain. Proc Natl Acad Sci U S A **93**, 3684-3688

187. Miledi, R. (1982) A calcium-dependent transient outward current in Xenopus laevis oocytes. Proc R Soc Lond B Biol Sci **215**, 491-497

188. Barish, M. E. (1983) A transient calcium-dependent chloride current in the immature Xenopus oocyte. J Physiol **342**, 309-325

189. Gomez-Hernandez, J. M., Stuhmer, W., and Parekh, A. B. (1997) Calcium dependence and distribution of calcium-activated chloride channels in Xenopus oocytes. J Physiol **502 (Pt 3)**, 569-574

190. Weisstaub, N., Vetter, D. E., Elgoyhen, A. B., and Katz, E. (2002) The alpha9alpha10 nicotinic acetylcholine receptor is permeable to and is modulated by divalent cations. Hear Res **167**, 122-135

191. Surprenant, A., Rassendren, F., Kawashima, E., North, R. A., and Buell, G. (1996) The cytolytic P2Z receptor for extracellular ATP identified as a P2X receptor (P2X7). Science **272**, 735-738

192. Kawashima, K., Fujii, T., Moriwaki, Y., and Misawa, H. (2012) Critical roles of acetylcholine and the muscarinic and nicotinic acetylcholine receptors in the regulation of immune function. Life Sci **91**, 1027-1032

193. Kawashima, K., and Fujii, T. (2003) The lymphocytic cholinergic system and its contribution to the regulation of immune activity. Life Sci **74**, 675-696

194. Mikulski, Z., Hartmann, P., Jositsch, G., Zaslona, Z., Lips, K. S., Pfeil, U., Kurzen, H., Lohmeyer, J., Clauss, W. G., Grau, V., Fronius, M., and Kummer, W. (2010) Nicotinic receptors on rat alveolar macrophages dampen ATP-induced increase in cytosolic calcium concentration. Respir Res **11**, 133

195. Coddou, C., Yan, Z., Obsil, T., Huidobro-Toro, J. P., and Stojilkovic, S. S. (2011) Activation and regulation of purinergic P2X receptor channels. Pharmacol Rev **63**, 641-683

196. Bo, X., Zhang, Y., Nassar, M., Burnstock, G., and Schoepfer, R. (1995) A P2X purinoceptor cDNA conferring a novel pharmacological profile. FEBS Lett **375**, 129-133

197. Buell, G., Lewis, C., Collo, G., North, R. A., and Surprenant, A. (1996) An antagonist-insensitive P2X receptor expressed in epithelia and brain. EMBO J **15**, 55-62

198. Jones, C. A., Chessell, I. P., Simon, J., Barnard, E. A., Miller, K. J., Michel, A. D., and Humphrey, P. P. (2000) Functional characterization of the P2X(4) receptor orthologues. Br J Pharmacol **129**, 388-394

199. Yan, Z., Liang, Z., Tomic, M., Obsil, T., and Stojilkovic, S. S. (2005) Molecular determinants of the agonist binding domain of a P2X receptor channel. Mol Pharmacol **67**, 1078-1088

200. Nakazawa, K. (1994) ATP-activated current and its interaction with acetylcholine-activated current in rat sympathetic neurons. J Neurosci **14**, 740-750

201. Searl, T. J., Redman, R. S., and Silinsky, E. M. (1998) Mutual occlusion of P2X ATP receptors and nicotinic receptors on sympathetic neurons of the guinea-pig. J Physiol **510 (Pt 3)**, 783-791

202. Khakh, B. S., Fisher, J. A., Nashmi, R., Bowser, D. N., and Lester, H. A. (2005) An angstrom scale interaction between plasma membrane ATP-gated P2X2 and alpha4beta2 nicotinic channels measured with fluorescence resonance energy transfer and total internal reflection fluorescence microscopy. J Neurosci **25**, 6911-6920